

Adequacy of Effective Born for electroweak effects and TauSpinner algorithms for LEP, Tevatron, HL-LHC and FCC simulated samples.

E. Richter-Was^a and Z. Was^b

^a *Institute of Physics, Jagellonian University, ul. Łojasiewicza 11, 30-348 Kraków, Poland*

^b *IFJ-PAN, 31-342, ul. Radzikowskiego 152, Kraków, Poland*

ABSTRACT

Matching and comparing the measurements of past and future experiments calls for consistency checks of calculations used for their interpretation. On the other hand, new calculation schemes of the field theory can be beneficial for precision, even if they may obscure comparisons with earlier results. Over the years concepts of *Improved Born*, *Effective Born*, as well as of effective couplings, in particular of $\sin^2 \theta_W^{eff}$ mixing angle for electroweak interactions, have evolved.

In our discussion we use four DIZET electroweak library versions; that of today and of the last 30 years. They were used for phenomenology of practically all HEP accelerator experiments. Versions differ by incremental updates of certain types of corrections which became available with time. We rely on the codes published and archived with the KKMC Monte Carlo program for $e^+e^- \rightarrow f\bar{f}n(\gamma)$. All these versions became recently available for the TauSpinner algorithm of simulated event reweighting as well. Such reweighting can be performed after events are generated and stored in data files. To this end DIZET is first invoked, and its results are used. Documentation of TauSpinner upgrade, to version 2.1.0, and of its arrangement for semi-automated electroweak effects benchmark plots are provided. Some details of the tool, which can be used to complete simulation sample with electroweak effects, are given.

Focus is placed on the numerical results, on the different approximations introduced in Improved Born to obtain Effective Born, suited better to match with QCD corrections. The τ lepton polarization P_τ , forward backward asymmetry A_{FB} and parton level total cross section σ^{tot} are used to monitor the size of electroweak effects and effective $\sin^2 \theta_W^{eff}$ picture limitations for precision physics. Collected results include: (i) feasibility of *Effective Born* approximation and $\sin^2 \theta_W^{eff}$, (ii) differences between versions of electroweak libraries and (iii) parametric ambiguities due to e.g. m_t or $\Delta\alpha_h^{(5)}(s)$. These results can be considered as examples only, but allow one to evaluate the adequacy of *Effective Born* with respect to *Improved Born*. Definitions are addressed too.

IFJ-PAN-IV-2020-10 December 2020

This project was supported in part from funds of Polish National Science Centre under decisions DEC-2017/27/B/ST2/01391.

Partly supported by the CERN FCC Design Study Program. Majority of the numerical calculations were performed at the PLGrid Infrastructure of the Academic Computer Centre CYFRONET AGH in Krakow, Poland.

1 Introduction

One of precision high energy physics great achievements in electroweak (EW) sector measurements is establishing that quantum field theory can be indeed used to calculate predictions that match measurement predictions [1, 2]. To handle results and interpretation, the concept of idealized observables was very useful [3]. Over many years the effective EW mixing angle $\sin^2 \theta_W^{eff}$ (of the process $e^+e^- \rightarrow Z/\gamma^* \rightarrow f\bar{f}$, where f denote leptons or quarks) was a prime candidate to evaluate sensitivity of observations of the EW sectors and in fact established itself as the idealized observable [2]. This universal quantity is not of the principal nature and to remain useful, confirmation that the necessary approximation still holds is needed. Already in the past, limits for the validity of the assumptions made were investigated. Let us point to an early reference [4], where dependence on flavour and the flavour-dependent $\sin^2 \theta_W^{eff}$ were elaborated.

In the calculation scheme used in LEP times, EW corrections calculated at one-loop level were improved with selected, dominant higher order terms and embedded in the Improved Born Approximation [5]. This formulation was a cornerstone for LEP measurements [1]. The Effective Born means redefining coupling constants to the values incorporating dominant contributions from the higher order (loop) corrections (at fixed energy, e.g. \sqrt{s} or M_Z). Such a redefinition usually does not break properties required for factorizing out calculation of strong interaction effects. In contrary, Improved Born where couplings are accompanied with energy- and angle-dependent, complex form-factors if used directly, can easily damage strong interaction gauge invariance and force the necessity of simultaneous calculation of the EW and QCD effects, without conveniences of factorization. The effective coupling definitions rely on properties of EW loop corrections, which could invalidate the concept of Effective Born and $\sin^2 \theta_W^{eff}$ definition as well. The concept has evolved over time [6, 7, 8]. In fact, approach variants, the controversies and differences in conventions can be now easily identified and avoided. One should keep in mind that such conventions were used in data analyzes of the past. With the improving measurements precision, one has to readdress the validity of assumptions and approximations necessary for definitions and usefulness of Effective and Improved Born.

To address the above points one needs to investigate first if Improved or Effective Born can be separated with sufficient precision from complete calculations including strong interactions. References [9, 10] were devoted to studying how the strong interaction separates in LHC processes of W and Z boson production and decay. The study was necessary for validation of `TauSpinner` event reweighting algorithm [11, 12] in its implementation of EW effects [13]. Similar evaluations were completed in the past for e^+e^- collisions in context of Monte Carlo generators [14, 15, 16] and for semi-analytical calculations in [5]. One of the important numerical assumptions was that in all these applications, numerical differences between Improved and Effective Born are, around the Z pole, not too large. The one-loop genuine weak corrections were usually calculated for all these projects with the help of `DIZET` library [17]. Important was the inclusion of some higher order strong interaction or QED effects. One has always to check if necessary higher order contributions to weak loop effects can be (and are) introduced into Effective or Improved Born and thus partly re summed as well. For `DIZET` archivization and evolution see Ref. [18] and references therein.

Obviously, whenever precision is expected to improve, assumptions behind calculations need to be revisited. The `TauSpinner` algorithms can be helpful in that respect and used to evaluate if for a given observable some classes of the corrections are necessary or can be ignored. Independently if old calculations are sufficient or if the new one may be necessary, it is useful to establish which of the effects need to be taken into account.

We focus on discussion/evaluation of: (i) the suitability of Effective versus Improved Born approximation (also the usefulness of $\sin^2 \theta_W^{eff}$), (ii) differences between results of `DIZET` library versions in use over the last 30 years, (iii) ambiguities due to parametric uncertainties or due to (sometimes) missing contributions. We explain minor, but useful for studies of EW effects, `TauSpinner` extensions with respect to Ref. [13], too.

In the scope of the paper, we present numerical results, either from semi-analytical calculations (predominantly for $e^+e^- \rightarrow l^+l^-$ processes) or from reweighting of the Monte Carlo event samples (predominantly for $pp \rightarrow Z/\gamma^* \rightarrow l^+l^-$ processes at 8 TeV center of mass collisions). In the second case we use Powheg Monte Carlo $Z + jets$ events as described in Refs. [9, 13].

Section 2 recalls basic definitions necessary for the introduction of the Improved Born practical comments on $\sin^2 \theta_W^{eff}$ definitions are provided. Simplifications enabling introduction of Effective Born are explained as well. The purpose of Section 3 is to recall first numerical results on non-EW effects which are instrumental for the concept of Effective Born and effective couplings. Both Improved Born and Effective Born require interpolation of the $2 \rightarrow 2$ kinematics and evaluation of its scattering angle. This requires careful optimization in the presence of QED/QCD initial and final state emissions; see references above, which discuss the issue. In this context, redefinitions of couplings are convenient as such couplings can be usually used in strong interactions amplitudes without complication of gauge dependence restoration. Alternatively, re-weighting to Improved Born can be advocated following e.g. the `TauSpinner` solution of Ref. [13]. The particular choice will need to be decided by the user precision requirements. That is why we do not give any guidelines here. Definitions of simplified test observables used all over the paper are provided.

Section 4 is devoted to the comparison of Improved Born and Effective Born. In particular, results useful to evaluate precision of Effective Born and $\sin^2 \theta_W^{eff}$ approximations with respect to Improved Born are provided. Most of the numerical details, are delegated to Appendices. Ref. [18] summarizes numerically most important upgrades of EW library `DIZET`. Some

numerical comparisons of its variants are collected in Section 5. Numerical results for parametric uncertainties are given in Subsection 5.1. Summary, Section 6, closes the paper.

Technical and physics content details of `DIZET` library versions, including used by us in these cases initialization parameters are collected in Appendix A. Alternative EW projects and calculation schemes are not discussed and we address interested readers to the documentation of `KKMC` [15] or even older `KORALZ` documentation [14]. Appendix B supplements the paper with technical details on the `TauSpinner` re-weighting algorithm. Details of variants of Born definitions and activating them flags available in `TauSpinner` are given in Appendix C. Appendix D addresses the important but auxiliary point of the Z propagator with running or fixed width and provides corresponding numerical results. Appendix E enumerates versions of `DIZET` library, which are available from Ref. [18].

2 Improved Born and electroweak form-factors.

In the Improved Born Approximation, the complete $O(\alpha)$ EW corrections, supplemented by selected higher order terms, are handled with form-factor corrections, dependent on (s, t) , multiplying couplings and propagators of the usual Born expressions. Let us continue with definition of Improved Born used in `TauSpinner`. It is detailed in Ref. [13] but we will recall it with Eq. (1) for the process $e^+e^- \rightarrow f\bar{f}$. The formula can be used also in the case when initial and final state are interchanged. The z component of the fermion isospin $T_3^{e,f}$, EW mixing angle $s_W^2 = \sin^2 \theta_W$, $c_W^2 = 1 - s_W^2$ and electric charge $q_{e,f}$ are used, as usual, for the coupling constant calculations. The Mandelstam variables $s = (p_{e^+} + p_{e^-})^2$ and $t = (p_f - p_{e^-})^2$ are used for the kinematical dependence. The Fermi coupling G_μ , QED coupling constant α , the Z boson mass M_Z and width Γ_Z complete basic notations. Definitions of EW form-factors $K_e(s, t), K_f(s, t), K_{ef}(s, t)$, for $\ell = e, \mu, \tau$, photon vacuum polarization $\Pi_\gamma(s)$ and $\rho_{\ell f}(s, t)$, are as used in [13]. It is important that they are only weakly dependent on t , and the s dependence is not sizable as well¹.

$$ME_{Born+EW} = \mathcal{N} \frac{\alpha}{s} \left\{ [\bar{u}\gamma^\mu v g_{\mu\nu} \bar{v}\gamma^\nu u] \cdot (q_e \cdot q_f) \cdot \Gamma_{V\Pi} \cdot \chi_\gamma(s) \right. \\ \left. + [\bar{u}\gamma^\mu v g_{\mu\nu} \bar{v}\gamma^\nu u \cdot (v_e \cdot v_f \cdot v v_{ef}) + \bar{u}\gamma^\mu v g_{\mu\nu} \bar{v}\gamma^\nu \gamma^5 u \cdot (v_e \cdot a_f) \right. \\ \left. + \bar{u}\gamma^\mu \gamma^5 v g_{\mu\nu} \bar{v}\gamma^\nu u \cdot (a_e \cdot v_f) + \bar{u}\gamma^\mu \gamma^5 v g_{\mu\nu} \bar{v}\gamma^\nu \gamma^5 u \cdot (a_e \cdot a_f)] \cdot Z_{V\Pi} \cdot \chi_Z(s) \right\}, \quad (1)$$

$$\begin{aligned} v_e &= (2 \cdot T_3^e - 4 \cdot q_e \cdot s_W^2 \cdot K_e(s, t)) / \Delta, \\ v_f &= (2 \cdot T_3^f - 4 \cdot q_f \cdot s_W^2 \cdot K_f(s, t)) / \Delta, \\ a_e &= (2 \cdot T_3^e) / \Delta, \quad s_W^2 = (1 - c_W^2) = 1 - M_W^2 / M_Z^2, \\ a_f &= (2 \cdot T_3^f) / \Delta, \quad \Delta = 4 s_W c_W, \\ \chi_Z(s) &= \frac{G_\mu \cdot M_Z^2 \cdot \Delta^2}{\sqrt{2} \cdot 8\pi \cdot \alpha} \cdot \frac{s}{s - M_Z^2 + i \cdot \Gamma_Z \cdot s / M_Z}, \\ \Gamma_{V\Pi} &= \frac{1}{2 - (1 + \Pi_\gamma(s))}, \quad Z_{V\Pi} = \rho_{\ell f}(s, t), \quad \chi_\gamma(s) = 1, \\ v v_{ef} &= \frac{1}{v_e \cdot v_f} [(2 \cdot T_3^e)(2 \cdot T_3^f) - 4 \cdot q_e \cdot s_W^2 \cdot K_f(s, t) - 4 \cdot q_f \cdot s_W^2 \cdot K_e(s, t) \\ &\quad + (4 \cdot q_e \cdot s_W^2)(4 \cdot q_f \cdot s_W^2) K_{ef}(s, t)] \frac{1}{\Delta^2}. \end{aligned}$$

In the formula u, v stand for spinors - fermions wave functions, and \mathcal{N} is a normalization factor which is convention dependent (e.g. for wave functions normalization).

The formula (1) is not the only possibility for implementation of EW corrections. Genuine EW corrections can be, under some conditions, combined with the ones of QED or strong interactions. For example in `KKMC` implementation, the Improved or Effective Born approximation is not used. EW form-factors are installed into spin amplitudes directly². Care of the gauge

¹At the LO EW $K_e(s, t) = K_f(s, t) = \rho_{\ell f}(s, t) = 1$, $\Pi_\gamma(s) = 0$ and $\frac{G_\mu M_Z^2 \Delta^2}{\sqrt{2} 8\pi \alpha} = 1$. We use $s_W^2 = 1 - M_W^2 / M_Z^2$ for the on-mass-shell definition, while $\sin^2 \theta_W^{eff}$ is used for the effective value corresponding to the ratio of couplings at the Z -pole $v_f^{eff} / a_f^{eff} = 1 - 4 q_f \sin^2 \theta_W^{eff}$.

²That could be disastrous, as gauge cancellations would be broken. Spinor techniques of Kleiss-Stirling [19] are exploited for `KKMC` Monte Carlo of $e^+e^- \rightarrow l^+l^- n\gamma$ processes, where second order QED matrix element and coherent exclusive exponentiation is used [16, 15]. Nonphysical huge contributions proportional even to $\sim 1/m_e^2$ could appear. However this is not the case as contributions to Yennie Frautchi Suura spin amplitude level β_0, β_1, \dots terms are

cancellation was essential for that. The “running” of Γ_Z for the $\chi_Z(s)$ propagator is used in Eq. (1) as was commonly the case for LEP physics, but less so for LHC oriented MC’s. Another possibility is to use Effective Born (not exact at one loop level, it will be discussed in Section 3.1). The main idea is to simplify formula (1). In particular, include in $\sin^2 \theta_W^{eff}$ the bulk effect of $K_e(s, t)$ and $K_f(s, t)$ form-factors present in front of s_W^2 , and vacuum polarization corrections Π_γ into a redefinition of α . In fact a real part or a module, and all calculated at the Z pole. It is also possible to think of $\sin^2 \theta_W^{eff}$ as the best result of the fit to the data. At certain precision level, such distinction may start to play a role and one should be aware of alternatives to avoid misunderstandings.

Definitions of form-factors follows the one of the `DIZET` library [17, 18] and are as used for spin amplitudes in the `KKMC` Monte Carlo as well. For convenience they are used in the Improved Born, formula (1), of `TauSpinner` too. Details of the EW scheme, initialization parameters are provided in Appendix A. In Fig. 1 EW form-factors calculated with `DIZET` library are drawn.

A disadvantage of the Improved Born with respect to the Effective one is that it is not immediate to merge its formulation into calculations for strong interactions. Formula (1) can be used as a starting point to explain relations between Improved Born and Effective Born, where s - and t -dependent form-factors are avoided. For the latter, form-factors are often set to unity, but may be replaced with the real constants without compromising strong interaction calculations. One should keep in mind that numerical values for e.g. s_W^2 and α need then to be chosen differently, also to accumulate dominant numerical contributions of the loop corrections. Technical details for the arrangements used in the programs are collected in Table 12 of the Appendix C.

3 Factorization requirements for Born amplitudes

In the general case, but especially for lepton pair production at the LHC, the definition and use of the quark $2 \rightarrow 2$ Born-level scattering process as a building block for phenomenology, may seem rather crude and difficult to control. Let us recall arguments why it is not necessarily the case.

Properties of Born-level spin amplitudes lead to features necessary for its factorization from complete formulae. Quality of such separation is of a decisive importance. Already a long time ago [20], even in the presence of hard bremsstrahlung photons, the part of amplitudes which corresponds to the Born-level distribution were identified and separated out. This was studied in the context of hadronic kinematic configuration of pp LHC physics as well [9, 10] and for configurations with up to two high p_T jets. These factorization properties were expected, thanks to e.g. results of [21]. They require that the Born cross section is described by spherical harmonics of the second order. Indeed, the Born cross section for $f\bar{f} \rightarrow Z/\gamma^* \rightarrow \ell^+\ell^-$ reads (azimuthal angle dependence can be avoided with appropriate choice of the reference frame):

$$\frac{d\sigma_{Born}^{q\bar{q}}}{d\cos\theta}(s, \cos\theta, p) = (1 + \cos^2\theta) F_0(s) + 2\cos\theta F_1(s) - p[(1 + \cos^2\theta) F_2(s) + 2\cos\theta F_3(s)], \quad (2)$$

where p denotes polarization of the outgoing leptons, θ an angle between incoming quark and outgoing lepton in the rest frame of outgoing leptons. For a general orientation of the reference frame all second order spherical harmonics in θ and ϕ angles appear. Second order spherical harmonics are sufficient also when transverse spin effects are taken into account.

The F_i read:

$$\begin{aligned} F_0(s) &= \frac{\pi\alpha^2}{2s} [q_f^2 q_\ell^2 \cdot \chi_f^2(s) + 2 \cdot \chi_f(s) \text{Re}\chi_Z(s) q_f q_\ell v_f v_\ell + |\chi_Z(s)|^2 (v_f^2 + a_f^2)(v_\ell^2 + a_\ell^2)], \\ F_1(s) &= \frac{\pi\alpha^2}{2s} [2\chi_f(s) \text{Re}\chi(s) q_f q_\ell v_f v_\ell + |\chi^2(s)|^2 2v_f a_f 2v_\ell a_\ell], \\ F_2(s) &= \frac{\pi\alpha^2}{2s} [2\chi_f(s) \text{Re}\chi(s) q_f q_\ell v_f v_\ell + |\chi^2(s)|^2 (v_f^2 + a_f^2) 2v_\ell a_\ell], \\ F_3(s) &= \frac{\pi\alpha^2}{2s} [2\chi_f(s) \text{Re}\chi(s) q_f q_\ell v_f v_\ell + |\chi^2(s)|^2 (v_f^2 + a_f^2) 2v_\ell a_\ell], \end{aligned} \quad (3)$$

Unfortunately with s, t -dependent EW form-factors of Eq. (1), the assumption on spherical harmonics decomposition of the second order only does not hold. Inevitably the approximation needs to be re-checked if it matches the required precision. Checks if approximations do not deteriorate precision sizably, can be obtained from semi-analytical calculation or from fits of re-weighted events distributions. For many applications it is sufficient to realize that an assumption of angle independent form-factors works well at the vicinity of the Z peak. This can be observed for form-factors presented in Fig. 1: lines corresponding to distinct scattering angles cross all at about $\sqrt{s} = M_Z$. This observation may be not always sufficient. If off

calculated explicitly and gauge cancellations are explicitly performed, before EW form-factors installation.

One needs to keep in mind this difficulty when other applications are developed. Even in `KKMC` case this needed to be watched after, in the context of e.g. IFI interference contribution, where cancellation of real and virtual corrections play a role and may be obscured by energy angular dependence of form-factors. Formally of higher order, such mismatches could substantially impact conclusions if attention was not paid.

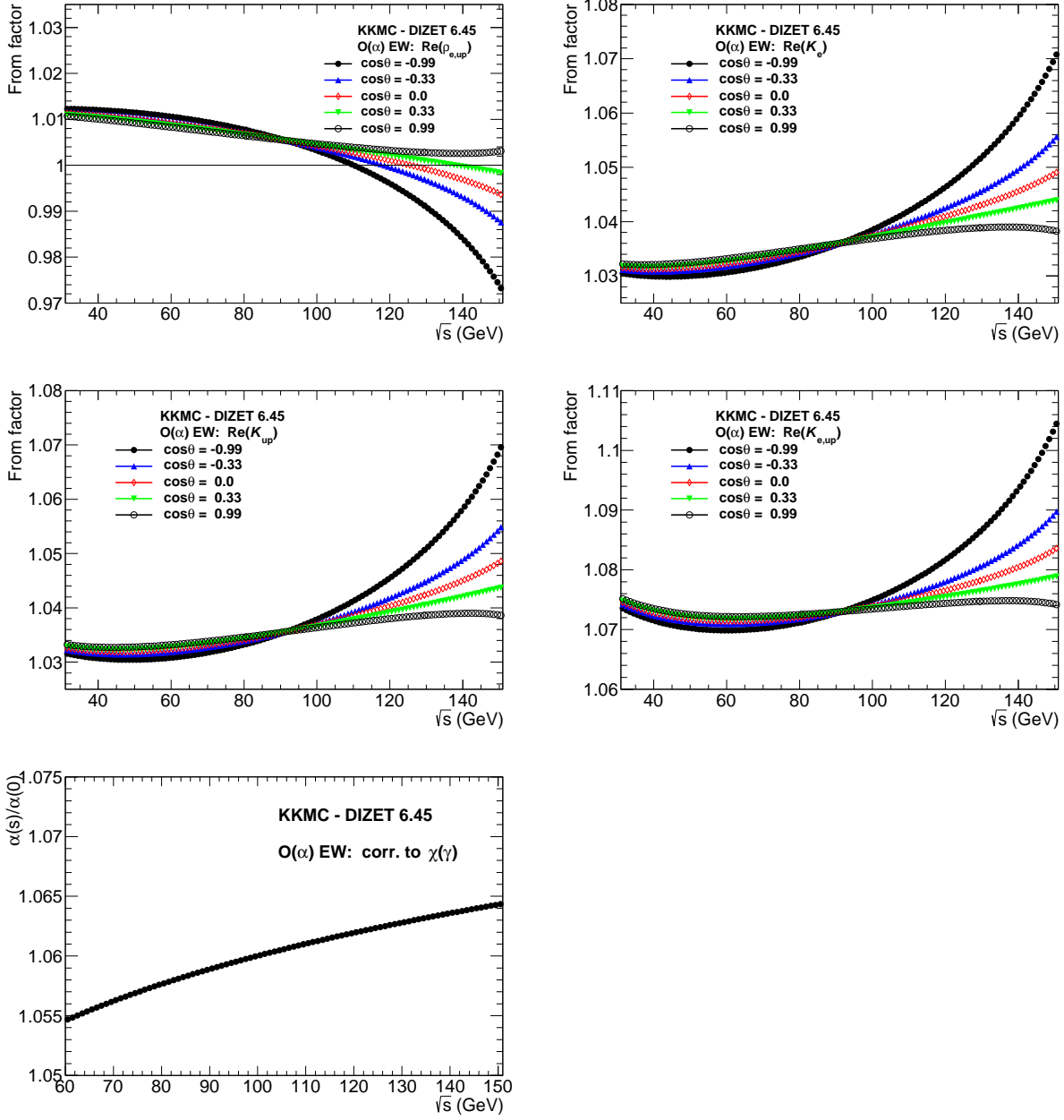


Figure 1: Plots from the new `examples/Dizet-example` directory of TauSpinner. The real parts of the $\rho_{e,up}$, \mathcal{K}_e , \mathcal{K}_{up} and $\mathcal{K}_{e,up}$ EW form-factors of $ee \rightarrow Z \rightarrow u\bar{u}$ process, as a function of \sqrt{s} and for the few values of $\cos\theta$. Note, that $\mathcal{K}_{e,up}$ depends on the flavour of outgoing quarks. On the last plot (bottom line) the ratio $\alpha(s)/\alpha(0) = \Gamma_{V_H}$ is also shown.

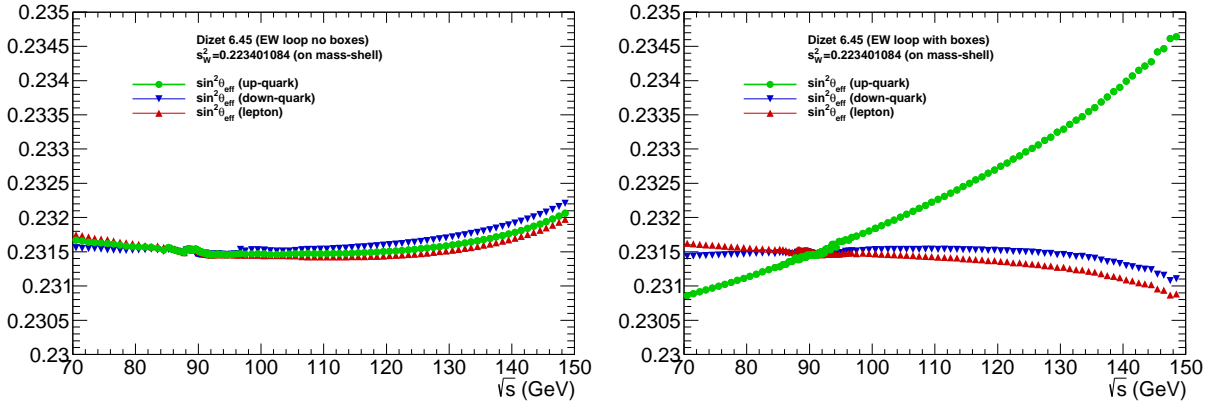


Figure 2: Averaged for $pp \rightarrow Zj$, $Z \rightarrow l\bar{l}$ events effective weak mixing angles $\sin^2 \theta_W^{eff}(s) = \text{Re}(K^f(s, t)) s_W^2$ as a function of \sqrt{s} and t -dependence integrated over, without (left-hand plot) and with (right-hand plot) box corrections. The $\mathcal{K}^f(s, t)$ form-factor calculated using DIZET 6.45 library and on-mass-shell $s_W^2 = 0.223401084$ were used (see Table 4). The complete formula reads $\sin^2 \theta_W^{eff}(s, t) = K^f(s, t) s_W^2 + I_f^2(s, t)$. Real part of $K^f(s, t)$ is used, imaginary part and $I_f^2(s, t)$ are only about 10^{-4} .

peak contributions to the observable of interest are sizable, then checks with figures indicating the range of \sqrt{s} contributing to observables need to be evaluated. To estimate, e^+e^- , or parton level, total cross sections and asymmetries, like presented later in Fig. 3, may be used. The $\sin^2 \theta_W^{eff}$ represents a typical observable and/or coupling constant. That is why Fig. 2 of \sqrt{s} and flavour-dependent $\sin^2 \theta_W^{eff}$ provides a hint on the size of the effect as well. For t -dependence, EW boxes contribute with correction of isospin dependent sign. On the other hand, the $\sin^2 \theta_W^{eff}$ variations remain below $20 \cdot 10^{-5}$ in the range of $M_Z \pm 5$ GeV. The t -dependence originating from WW and ZZ boxes becomes sizable once s approaches $4M_W^2$, the W -pair production threshold.

Note that even if for a given observable the nearby of the Z peak dominates for LEP (or even FCC), this may not be the case for LHC or linear colliders. There, off Z peak contributions are larger due to PDF or beamstrahlung spread. This needs to be kept in mind, in context of the $\sin^2 \theta_W^{eff}$ interpretation as universal idealized observable. We recall that off the Z peak form-factors dependence on flavour and scattering angle increase, see Fig. 1. It is therefore of interest to validate the range where form-factors angle and energy dependence can be safely ignored and the Effective Born Approximation used.

3.1 Improved Born Approximation and Effective Born

In principle it is not possible to absorb fully the effects of EW form-factors of Eq. (1) (which are all complex and angle/energy dependent) into rescaling of constants. In particular, introduction of $\sin^2 \theta_W^{eff}$ is prone to complications and ambiguities (see footnote¹ earlier in the text). Let us now recall details of Effective Born amplitude definition, which differs from formula (1): the form-factors are replaced by effective coupling constants (see also Table 12 of Appendix C).

$$\begin{aligned}
 ME_{\text{Born-eff}} = \mathcal{N}_s^{\frac{g}{s}} \{ & [\bar{u}\gamma^\mu v g_{\mu\nu} \bar{v}\gamma^\nu u] \cdot (q_e \cdot q_f) \cdot \Gamma_{V_H} \cdot \chi_\gamma(s) \\
 & + [\bar{u}\gamma^\mu v g_{\mu\nu} \bar{v}\gamma^\nu u \cdot (v_e \cdot v_f \cdot v v_{ef}) + \bar{u}\gamma^\mu v g_{\mu\nu} \bar{v}\gamma^\nu \gamma^5 u \cdot (v_e \cdot a_f) \\
 & + \bar{u}\gamma^\mu \gamma^5 v g_{\mu\nu} \bar{v}\gamma^\nu u \cdot (a_e \cdot v_f) + \bar{u}\gamma^\mu \gamma^5 v g_{\mu\nu} \bar{v}\gamma^\nu \gamma^5 u \cdot (a_e \cdot a_f)] \cdot Z_{V_H} \cdot \chi_Z(s) \}
 \end{aligned} \tag{4}$$

$$\begin{aligned}
v_e &= (2 \cdot T_3^e - 4 \cdot q_e \cdot s_W^2) / \Delta \\
v_f &= (2 \cdot T_3^f - 4 \cdot q_f \cdot s_W^2) / \Delta \\
a_e &= (2 \cdot T_3^e) / \Delta, \quad \Delta = 4s_W c_W \\
a_f &= (2 \cdot T_3^f) / \Delta, \quad \chi_Z(s) = \frac{G_\mu \cdot M_Z^2 \cdot \Delta^2}{\sqrt{2} \cdot 8\pi \cdot \alpha} \cdot \frac{s}{s - M_Z^2 + i \cdot \Gamma_Z \cdot s / M_Z}, \\
\Gamma_{V\Pi} &= 1, \quad Z_{V\Pi} = \text{Re} \rho_{\ell f}(M_Z^2), \quad \chi_\gamma(s) = 1, \\
v_{\nu ef} &= 1, \quad s_W^2 = (1 - c_W^2) = \sin^2 \theta_W^{eff}(M_Z^2), \\
\alpha &= \alpha(M_Z^2) = \frac{\alpha(0)}{2 - (1 + \text{Re} \Pi_{\gamma\gamma}(M_Z^2))}.
\end{aligned}$$

Note that $\sin^2 \theta_W^{eff}(M_Z^2)$, $\rho_{\ell f}(M_Z^2)$ and $\alpha(M_Z^2)$ are now used. They absorb dominant parts of EW corrections; EW form-factors and vacuum polarization corrections. This useful approximation may take into account bulk of the EW effects, and couplings of fixed values are used. There is some level of ambiguity in the numerical values. The best match to Improved Born should correspond to the values predicted by these calculations. In particular, $\sin^2 \theta_W^{eff}(M_Z) = \text{Re} K(M_Z^2, -M_Z^2/2) s_W^2$, $s_W^2 = 1 - M_W^2/M_Z^2$, where M_W is a calculated quantity including EW corrections. The $s = M_Z^2$, $t = -M_Z^2/2$, corresponds to the Born-level with scattering angle $\theta = 0$. Alternatively, one could use best measured values [1, 2] and not rely on the EW calculations. This may be of importance for calculations which are focused, e.g., on strong interactions. Complications due to mixed EW and strong interaction loops in Feynman diagrams i.e. gauge dependence non-cancellation can be avoided. The price is precision limitation with respect to Improved Born. Such an approach was used for the previous Tauola/TauSpinner ME implementation, with $\sin^2 \theta_W^{eff}(M_Z)$, $\alpha(M_Z^2)$ as measured at LEP [2] and $\rho_{\ell f} = 1$ for simplification.

To monitor EW effects we use $e^+e^- (q\bar{q})$ to pair of leptons, parton level cross section σ^{tot} , forward-backward asymmetry A_{FB} and τ lepton polarization P_τ , as a function of \sqrt{s} .

The Z/γ^* -boson e^+e^- (or $q\bar{q}$) cross section σ^{tot} in the EW LO, depends only on coupling constants and two parameters (M_Z, Γ_Z). The effect on σ^{tot} from EW loop corrections are due to corrections to the propagators: vacuum polarization corrections (running α) and ρ form-factor. This causes a change in relative contributions of the Z and γ , and change of the Z -boson vector to axial coupling ratio ($\sin^2 \theta_W^{eff}$). They affect not only s -dependence but normalization of the cross section too.

The forward-backward asymmetry $A_{FB} = \frac{\sigma(\cos\theta>0) - \sigma(\cos\theta<0)}{\sigma(\cos\theta>0) + \sigma(\cos\theta<0)}$

is defined in a standard way. For e^+e^- collision, an angle θ between incoming particle and outgoing lepton is taken. For pp collision the *Collins-Soper* frame [22] is used for angle θ definition. The asymmetry varies strongly with \sqrt{s} around the Z peak because it is proportional to product of small vector v_i and v_f couplings of incoming parton and outgoing lepton. The product is specially small for e^+e^- initial state. That is why, off the peak, s -channel Z -photon exchange interference quickly become sizable.

The τ polarization $P_\tau = \frac{\sigma(R) - \sigma(L)}{\sigma(R) + \sigma(L)}$ where $\sigma(R/L)$ denote cross section for production of right/left hand polarized τ , is of interest in itself as it offers independent data-point for precision EW sector measurements. It is of convenience, because, in the first approximation, it is linearly proportional to $\sin^2 \theta_W^{eff} \tau$, thus it is useful for discussion of systematic ambiguities. The systematic errors for this measurement differ from that of σ^{tot} or A_{FB} . Predominantly because P_τ is not measured directly, but through distribution of τ decay products only. These points were recently recalled in [23]. On the other hand, relation between P_τ , Z couplings and $\sin^2 \theta_W^{eff}$ is not affected and generally is of the same nature like for A_{FB} . That is why this data point is particularly suitable for discussion with e^+e^- semi-analytical results.

Test observables and $\sin^2 \theta_W^{eff}$. It is worth to point out that of the e^+e^- scattering results, the ones for the P_τ are particularly convenient in discussion of $\sin^2 \theta_W^{eff}$. This is because P_τ is the linearly proportional to small vector Z -lepton coupling, thus to $\sin^2 \theta_W^{eff}$ itself. Also, the P_τ varies with energy in the vicinity of the Z peak relatively slowly. To a good approximation, as one can easily deduce from formula (4) any variation δ of P_τ measured at the Z peak translates into $\sim \frac{1}{8}\delta$ shift³ of $\sin^2 \theta_W^{eff}$ quite independently of the flavour of incoming state. This holds not only for e^+e^- but for incoming quarks too. For A_{FB} and σ^{tot} similar relations can be obtained, then ρ and α dependence would need to be taken into the picture. The initial state flavour and much stronger energy dependence would lead to multitude of cases. That is why we will use P_τ as an example to discuss suitability of the $\sin^2 \theta_W^{eff}$ picture and its limitations.

Fig. 3 for the e^+e^- case is shown for the start of numerical comparisons of Improved Born and Effective Born (TAUOLA/LEP initialization as specified later and installed in Tauola distribution) is shown. Differences are not large, but possibly not always satisfactory for precision physics. In fact TAUOLA/LEP Effective Born becomes insufficient for high precision measurements,

³At the Z peak $P_\tau \simeq \frac{2v_e}{a_e}$.

especially of hadron colliders (where off the Z peak contributions, contrary to the FCC, can not be minimized/excluded by the fixed colliding quark energies).

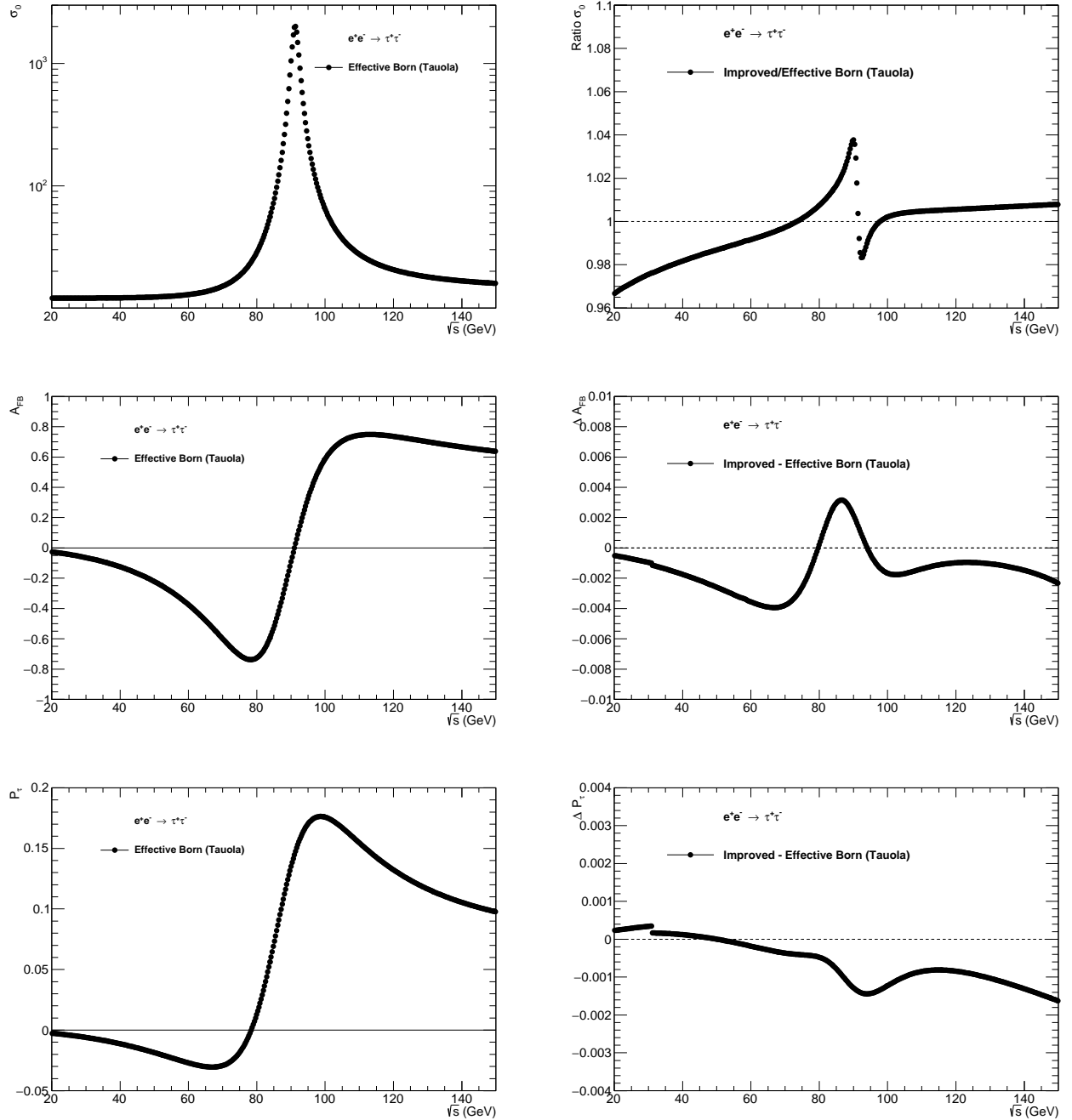


Figure 3: The $\sigma^{\text{tot}}(s)$, $A_{FB}(s)$ and $P_\tau(s)$ (left side, top, center and bottom plots respectively) of TauSpinner calculation with Effective Born (Tauola/LEP as installed in Tauola since December 2019). In the right side plots results of Improved Born calculations with EW form-factors from DIZET 6.45 are compared with those of the left side plots.

Note the differences depicted in the right side plots are enhanced in part because input parameters of Tauola/LEP initialization, see Table 1 for details. The M_Z and Γ_Z are slightly different than those used for Improved Born, causing sizable kink in the top right plot of σ^{tot} . On the right hand side plots there are minor discontinuities at 30 GeV, too. They are smaller than calculation precision and are due to granularity used for tabulation.

4 From Improved Born to Effective Born: numerical results.

Let us now attempt to identify those Effective Born simplifications which are of numerical consequences and those which are important from the theoretical perspective, but hopefully not so much numerically. The results will be compared to Improved Born results, which are the most precise ones. We keep all input parameters as of Improved Born but gradually simplify EW correcting terms.

It is helpful to test and to understand the impact of simplification steps from Improved \rightarrow Effective Born, on σ^{tot} , A_{FB} and P_τ and for all the elementary processes: $e^+e^- \rightarrow \tau^+\tau^-$ and $u\bar{u}(d\bar{d}) \rightarrow \tau^+\tau^-$. We concentrate on $e^+e^- \rightarrow \tau^+\tau^-$ process and choose for Figs. 4 and 5 the energy range important for the measurement of the Z boson couplings, that is $M_Z \pm 5$ GeV. The e^+e^- case is simpler to present and conclusions would not differ much if instead quark level processes would be used. For pp collisions, parton distribution functions would make discussions obscured, or unrealistic if dropped out. For reference results Improved Born and DIZET 6.45 EW library was used.

Approximation as of green points in Fig. 4 (marked “complex of Z peak”).

In this first step of approximation introduced into Eq. (1), the s - and t -dependent form-factors are replaced with their values at the Z peak and for the scattering angle $\cos\theta = 0$. One can see, that if constant complex couplings calculated at the Z peak instead of s, t -dependent form-factors are used, in the range of $M_Z \pm 5$ GeV the P_τ , A_{FB} and σ^{tot} departs from the exact result at the peak, respectively by up to $8 \cdot 10^{-5}$, $45 \cdot 10^{-5}$ and $40 \cdot 10^{-5}$. These largest differences are at the edge of the range, where cross section is already about a factor 20 smaller than at the peak.

If in addition $vv_{\ell f}$ was set to 1, additional changes are marginal. That is why in the Figure the case of $vv_{\ell f} = 1$ is not presented. Once $vv_{\ell f} = 1$ is set, mixing term is avoided and effective couplings are attributed separately to incoming and outgoing flavour.

Approximation as of blue triangles in Fig. 4 (marked as “real v , $vv=1$ ”).

The second step is to neglect imaginary parts of the vector couplings to Z . They are about factor of 100 smaller than the real parts. Now, the differences became larger, respectively up to $166 \cdot 10^{-5}$, $50 \cdot 10^{-5}$ and $32 \cdot 10^{-5}$. That means non-negligible degradation for P_τ , corresponding, in the language of $\sin^2\theta_W^{\text{eff}}$ to a $21 \cdot 10^{-5}$ prediction ambiguity.

Approximations as of red triangles and yellow stars in Fig. 4 (marked respectively “real Π_γ ” and “LEP2005 style”).

The role of the imaginary part of Π_γ requires special attention, particularly for A_{FB} . For red triangles, with respect to previous case, imaginary parts of Π_γ and $\rho_{\ell f}$ are set to zero, whereas for yellow stars, the imaginary part of $\rho_{\ell f}$ is set to zero only. The differences for “real Π_γ ” (“LEP 2005 style”) are respectively $152 \cdot 10^{-5}$, $188 \cdot 10^{-5}$, $32 \cdot 10^{-5}$, $(172 \cdot 10^{-5}, 60 \cdot 10^{-5}, 30 \cdot 10^{-5})$. The numerical effect of these imaginary parts, which can not be easily absorbed in redefinition of the couplings, need to be kept in mind.

With “LEP2005 style” parametrization we still do not address more subtle LEP time choices used in data analysis. In particular, of parametrisations used to separate contributions from s -channel exchange of Z boson and virtual photon exchange interfering background. In practice, in “LEP2005 style” variant, we use formula (1) but with $K_{e/f}(s, t) \rightarrow \text{Re}K_{e/f}(M_Z^2, -M_Z^2/2)$, $K_{e/f}(s, t) \rightarrow 1$, $\rho_{\ell f} \rightarrow \text{Re}\rho_{\ell f}(M_Z^2)$, that translates into use of flavour-dependent $\sin^2\theta_W^{\text{eff}}(M_Z^2)$. For $\alpha(M_Z^2)$ the replacement $\Pi_\gamma(s) \rightarrow \Pi_\gamma(M_Z^2)$ with a complex value is used. Now the purpose is to evaluate numerical consequences of $\alpha(s)$ ’s imaginary part. But it is also similar to what was used at a time of final precision data analysis of all LEP collaborations combined [2]. Motivations of the choices are discussed in Ref. [7]. The numerical impact is presented in Table 19 and is discussed in Section 5.4 of that reference, see also Section 5.4.4 of [2].

Figure 4 is accompanied with the extensive Table 14 in Appendix C. In total, results of eleven initializations variants are used for the Table. Of those, four are used in the figure. The variants, with gradually introduced simplifications to Improved Born EW corrections, were chosen. Most of the results were obtained with semi-analytic scripts of TauSpinner package, described in Appendix B. Details of the initializations are depicted in Table 13.

Our main observations:

(i) The Π_γ imaginary part, formally contributing at higher orders, was included in calculations for final LEP time data analysis. Its impact is largest for A_{FB} , whereas for P_τ imaginary parts of v_e , v_f couplings are more important. (ii) The form-factors replacement with constant effective couplings is numerically less important than when their imaginary parts are dropped. Also, the closer to the Z peak one goes, the smaller the disturbing of the Effective Born picture from photon exchanges. The same is true for the complex part of $\rho_{\ell f}$. Overall, numerical impact on observables is not universal and distinct sets of effective couplings might be needed for each of our test observables to match best the result of the Improved Born approximation.

4.1 The v_0 , v_1 , v_2 variants of Effective Born.

The formulae for Improved Born Eq. (1) and for Effective Born Eq. (4) differ with subtle, but numerically important details. We evaluate numerical effects again with the help of options in TauSpinner explained in Appendix C, in particular in Table 13.

One can ask the question how close can one approach Improved Born results, with the effective ones, without breaking features necessary for matching with calculations of strong interactions. Details of listed below variants for Effective Born

Table 1: The EW parameters used for: the EW LO Born in $\alpha(0)$ scheme, and for variants of effective Born. The $G_\mu = 1.1663887 \cdot 10^{-5} \text{ GeV}^{-2}$, $M_Z = 91.1876 \text{ GeV}$ ($M_Z = 91.1887 \text{ GeV}$ for Tauola/LEP) and $\mathcal{K}_f, \mathcal{K}_e, \mathcal{K}_{\ell f} = 1$.

Effective Born TAUOLA/LEP	EW LO $\alpha(0)$ scheme	Effective Born v0	Effective Born v1	Effective Born v2
$\alpha = 1/128.6667471$ $s_W^2 = 0.23152$ $\rho_{\ell f} = 1.0$	$\alpha = 1/137.03599$ $s_W^2 = 0.21215$ $\rho_{\ell f} = 1.0$	$\alpha = 1/128.9503022$ $s_W^2 = 0.231499$ $\rho_{\ell f} = 1.0$	$\alpha = 1/128.9503022$ $s_W^2 = 0.231499$ $\rho_{\ell f} = 1.005$	$\alpha = 1/128.9503022$ $s_W^{\ell} = 0.231499$ $s_W^{up} = 0.231392$ $s_W^{down} = 0.231265$ $\rho_{\ell up} = 1.005403$ $\rho_{\ell down} = 1.005889$

are provided in Table 1. Non-essential details are delegated to Appendix A. For completeness the reference starting points, TAUOLA/LEP parametrization and the EW LO Born parametrization in EW $\alpha(0)$ scheme, are provided. The consecutive three variants v0, v1, v2 of Effective Born are ordered with their ability to approximate better the *Improved Born* results, but at the same time, variants v1 and v2 may be less straightforward to implement into some programs designed for strong interaction in pp collisions.

- The v0 variant is using formula (4) for spin amplitude, with $\alpha(s) = \alpha(M_Z^2)$, $s_W^2 = \sin^2 \theta_W^{eff}(M_Z^2)$, but with $\rho_{\ell f} = 1.0$.
- The v1 variant is using formula (4) for spin amplitude, parameters are set as for v0 parametrization, but $\rho_{\ell f} \neq 1$.
- The v2 variant is using formula (4) for spin amplitude, parameters are set as if both s_W^2 and $\rho_{\ell f}$ were flavour-dependent, and equal at the Z-pole to the Dizet 6.45 predicted ones. See Table 1 and Table 4.
- The TAUOLA/LEP variant differs from v0 by numerical values of α , $s_W^2 = \sin^2 \theta_W^{eff}(M_Z^2)$. Also M_Z and Γ_Z differ. It is worth to point that Eq. (4) remains the same as for the Effective Born used at LEP 1 times.

Table 1 details v0, v1, v2 variants of *Effective Born*. Note that depending on the activated Born variant numerical values for $\sin^2 \theta_W^{eff}$, $\rho_{\ell f}$ and α may vary. The flavour dependence for $\sin^2 \theta_W^{eff}$ and $\rho_{\ell f}$ may appear, too.

We now present numerical results useful to evaluate robustness of the *Effective Born* picture, where effective couplings are used for describing EW effects, and compare it with results of the *Improved Born* picture. We will use *Improved Born* predictions as a reference for e^+e^- and $q\bar{q}$ cases⁴. As we will see, Effective Born v2 variant works quite well around the Z pole, for the line-shape and forward-backward asymmetry too. It may be not as straightforward to implement into strong interaction Monte Carlo programs as is the case of v0 or v1. That is why we will keep attention to all variants which differ numerically but may pose smaller or bigger problems for consistency of strong interaction calculations.

These Effective Born variants differ from Improved Born: constants instead of form-factors are used. This is partly compensated with adjustments of input parameters. In this way, in the following comparisons, we evaluate limits of $\sin^2 \theta_W^{eff}$ and Born-level EW formula for the interpretation of $Z-l-l$ couplings measurements.

Let us now turn our attention to numerical results. Fig. 5 is similar to Fig. 4 but serve different purpose. It enumerates the performance of v0, v1, v2 Effective Born with respect to the Improved Born. The shifts of v0 with respect to Improved Born respectively for P_τ , A_{FB} and σ^{tot} read $140 \cdot 10^{-5}$, $370 \cdot 10^{-5}$ and $1000 \cdot 10^{-5}$. This is already substantially better than EW at LO⁵. Obviously, normalization of the Z exchange needs to be corrected further. If $\rho_{\ell f}$ is used of variant v1, differences with respect to Improved Born reduce to: $140 \cdot 10^{-5}$, $200 \cdot 10^{-5}$ and $50 \cdot 10^{-5}$. With the v2 setting, reinstalling flavour dependence of couplings, we obtain results for the Effective Born which differ from the EW corrected ones by $140(40) \cdot 10^{-5}$, $200(40) \cdot 10^{-5}$ and $60(20) \cdot 10^{-5}$. Numbers in brackets were obtained with virtual γ contribution switched off⁶.

From these results, particularly for P_τ , we may conclude that approaches that rely on effective couplings may not work well for the $\sin^2 \theta_W^{eff}$ precision tag up to about $20 \cdot 10^{-5}$. For further improvement revisiting EW effects in their complexity is required. Use of numerically adapted Eq. (4) constants, which originally in Eq. (1) were multiplied by form-factors, does not

⁴In Appendix, Table 14, two versions of the *Improved Born* are used, with weak boxes included and not. This is important for large energy ranges. For e^+e^- we concentrate mostly on the region of the Z pole where the impact of EW boxes is marginal. We demonstrate the quantitative impact of the s, t -dependence, which can not be absorbed into effective couplings.

⁵If Effective Born v0 would be used, but with LO EW parameters the shifts on our tests observables with respect to Improved Born would be about a factor 100 larger.

⁶This hints that Effective Born may work better for pp collisions than for e^+e^- , because of smaller electric charge of quarks than of leptons.

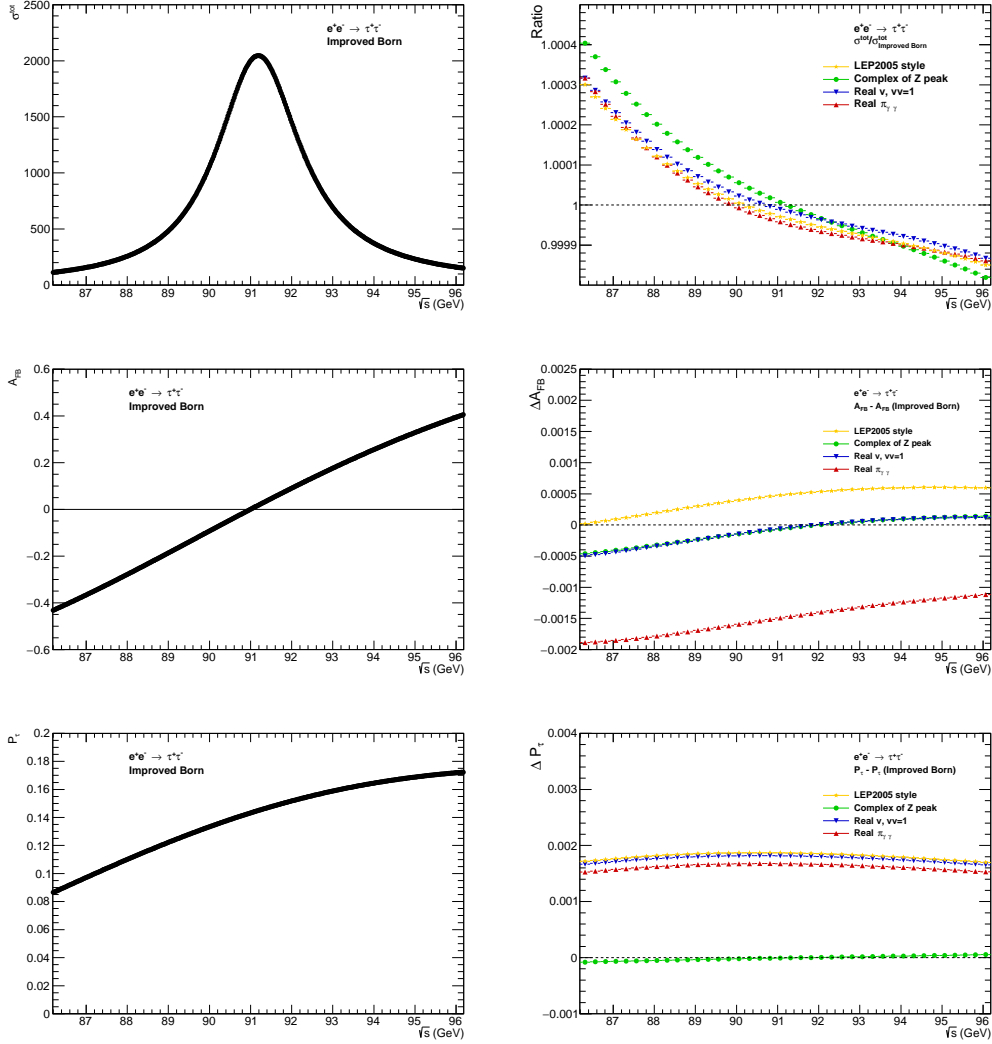


Figure 4: Left side plots, Improved Born-level and vicinity of the Z peak: σ^{tot} (top), A_{FB} (middle) and P_t (bottom). Right side plots enumerate, with ratios or differences the effects of simplifications with respect to Improved Born results. Green points: instead of form-factors, their constant values calculated at $s=M_Z^2$, $t=-M_Z^2/2$ are used. Blue triangles: as for green ones, but in addition $vv_{\ell f} = 1$ and only real parts of v_e, v_f are used. Red triangles: as in blue triangles, but only real parts of $\Pi_{\gamma\gamma}$ and $\rho_{\ell f}$ are taken into account. Yellow stars: with respect to red triangles imaginary parts of $\Pi_{\gamma\gamma}$ are switched back on.

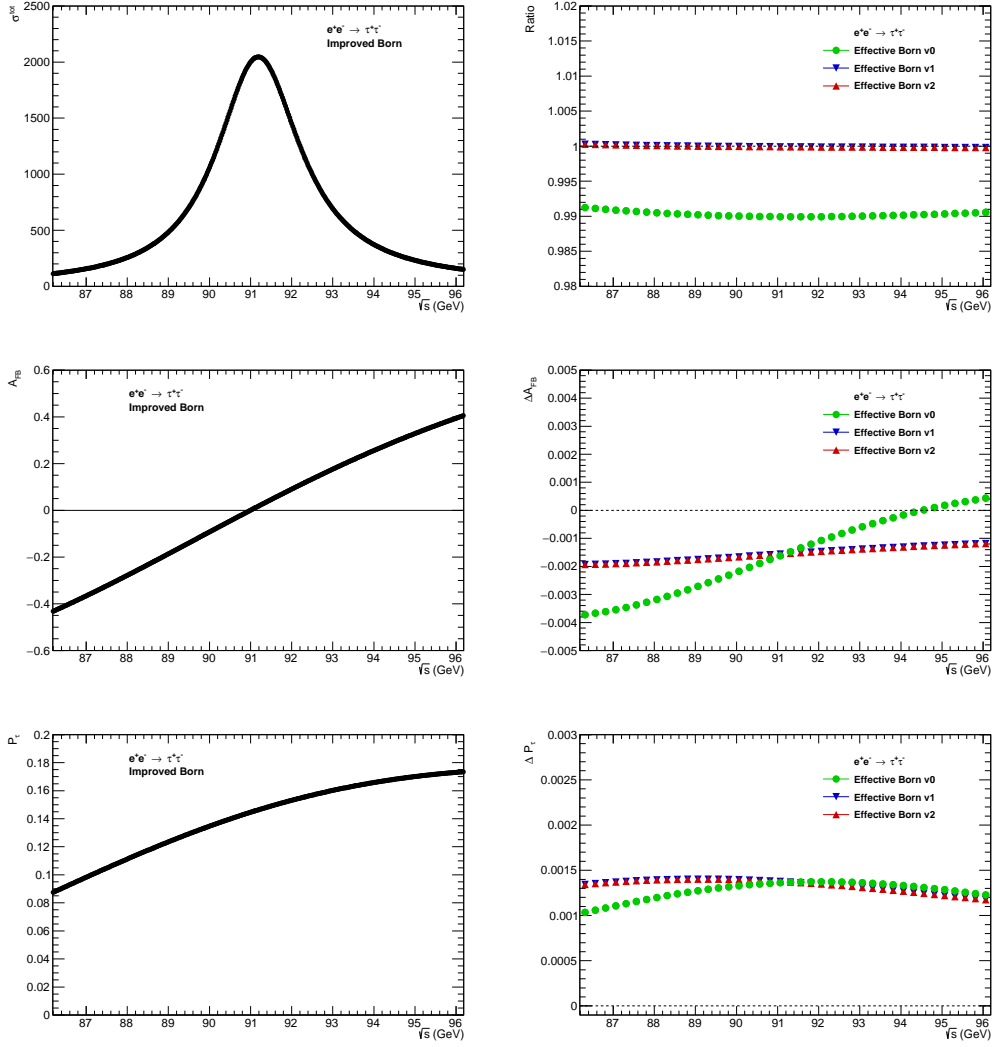


Figure 5: Left side plots, Improved Born in the vicinity of the Z peak: σ^{tot} (top), A_{FB} (middle) and P_t (bottom), as in Fig 4. Right side plots enumerate, with ratios or differences the effects of Effective Born simplifications with respect to Improved Born. Green points: Effective Born v0, Blue triangles: Effective Born v1 Red (rotated) triangles: Effective Born v2.

Table 2: EW corrections to cross sections σ^{tot} in the specified mass windows. DIZET 6.45 form-factors and running width was used in re-weighting of LHC $pp \rightarrow Zj$; $Z \rightarrow l^+l^-$ events simulated at 8 TeV. From the first two lines magnitude of EW corrections with respect to lowest order, $\alpha(0)$ scheme can be read off. Following three lines demonstrate precision of Effective Born variants with respect to Improved Born.

Corrections to cross section	$89 < m_{ee} < 93$ GeV	$81 < m_{ee} < 101$ GeV
$\sigma^{tot}(\text{Improved Born, no boxes})/\sigma(\text{EW LO } \alpha(0))$	0.96505	0.96626
$\sigma^{tot}(\text{Improved Born, with boxes})/\sigma(\text{EW LO } \alpha(0))$	0.96510	0.96631
$\sigma^{tot}(\text{Eff. Born } v0)/\sigma(\text{Improved Born, with boxes})$	1.01142	1.01135
$\sigma^{tot}(\text{Eff. Born } v1)/\sigma(\text{Improved Born, with boxes})$	1.00130	1.00132
$\sigma^{tot}(\text{Eff. Born } v2)/\sigma(\text{Improved Born, with boxes})$	0.99989	0.99987

suffice. For high precision, the picture of effective couplings is not universal: while appropriate for A_{FB} the choice may be not optimal for P_τ .

4.2 Case of $pp \rightarrow ll$ processes at LHC

Let us now discuss properties of these benchmark observables distributions and how numerically significant is change from Improved Born to the Effective Born approximation in the pp case contrary to e^+e^- , when semi analytic methods were applied simulated event sample and TauSpinner reweighting are used.

In Fig. 6 (top-left) distributions of generated and EW corrected Z-line-shape (through σ^{tot}) are shown for the pp collision case. The EW weight is calculated using $\cos\theta^*$ definition of the scattering angle as defined in [13]. On the logarithmic scale the difference is barely visible. In the following plots of the same figure we study it in more details. The ratios of the Z line-shape distributions with gradually introduced EW corrections are shown. We intend to evaluate the size of complete *Improved Born* predictions with respect to variants of *Effective Born*. That is why for reference predictions (denominator of the weights) the following: (i) EW LO $\alpha(0)$ (top-right plot), (ii) Effective Born $v0$ (bottom-left plot) and (iii) Effective Born $v2$ (bottom right plot), are used. For numerators, Improved Born of form-factors without/with box diagram contributions are used. At the Z-pole, complete EW corrections of Improved Born give for σ about 0.01% different results from the one of Effective Born $v2$. It demonstrates that if for event generation an EW LO matrix element is used with effective variant $v2$ parametrization, the size of missing EW effects will be significantly reduced.

Similar conclusions can be drawn from Table 2, where the numerical impact of EW corrections on the normalization i.e. ratios of the pp cross sections integrated in the range $81 < m_{ee} < 101$ GeV and $89 < m_{ee} < 93$ GeV, are given. Total EW corrections for EW LO $\alpha(0)$ cross section are about 0.035, while for the Effective Born $v0$ it is of about 0.01 and for Effective Born $v2$ is of about 0.0001. The main improvement of $v2$ with respect to $v0$ is thanks to $\rho_{lf} \neq 1$ introduced already for $v1$.

Let us now turn our attention to the EW corrections for the forward backward asymmetry A_{FB} . Again for the $pp \rightarrow Z/\gamma^* \rightarrow l^+l^-$ process, energy range from 60 to 150 GeV was chosen which is of interest for EW effects. As in the case of cross section, shape and size of the corrections depend on whether box exchange diagrams are included in the Improved Born result. In top-left plot of Fig. 7, the A_{FB} distribution, as generated (EW LO) and superimposed with EW corrected result is shown. The points for the two cases are practically indistinguishable. Further three plots of the figure, with the difference $\Delta A_{FB} = A_{FB} - A_{FB}^{ref}$ provide details. For the reference A_{FB}^{ref} , the three versions of the Effective Born detailed in Table 1 are used again: (i) EW LO $\alpha(0)$, (ii) $v0$ and (iii) $v2$. The EW corrections for A_{FB} of EW LO Born with $\alpha(0)$ scheme, integrated around the Z-pole, necessary to reproduce Improved Born result can reach -0.03514, see Tab. 3. The Effective Born $v0$ reproduces Improved Born up to ΔA_{FB} of about -0.0004, while the Effective Born $v2$ up to -0.0002. The $v2$ variant is again better by a factor of two than the $v0$ one.

All that points to the limitation of real constants Effective Born and its parametrization with $\sin^2 \theta_W^{eff}(M_Z)$ at about $20 \cdot 10^{-5}$ or so, even if $\alpha(M_Z)$ and $\rho_{lf}(M_Z)$ is used. Note that even if P_τ is not particularly suitable for pp collision measurements, it weakly depends on the production process and that is why it is suitable for numerical $\sin^2 \theta_W^{eff}(M_Z)$ ambiguities evaluation in general case. That is why previous subsection results are of the relevance for pp too. It is worth noting that they also point to $20 \cdot 10^{-5}$ as an ultimate precision tag,

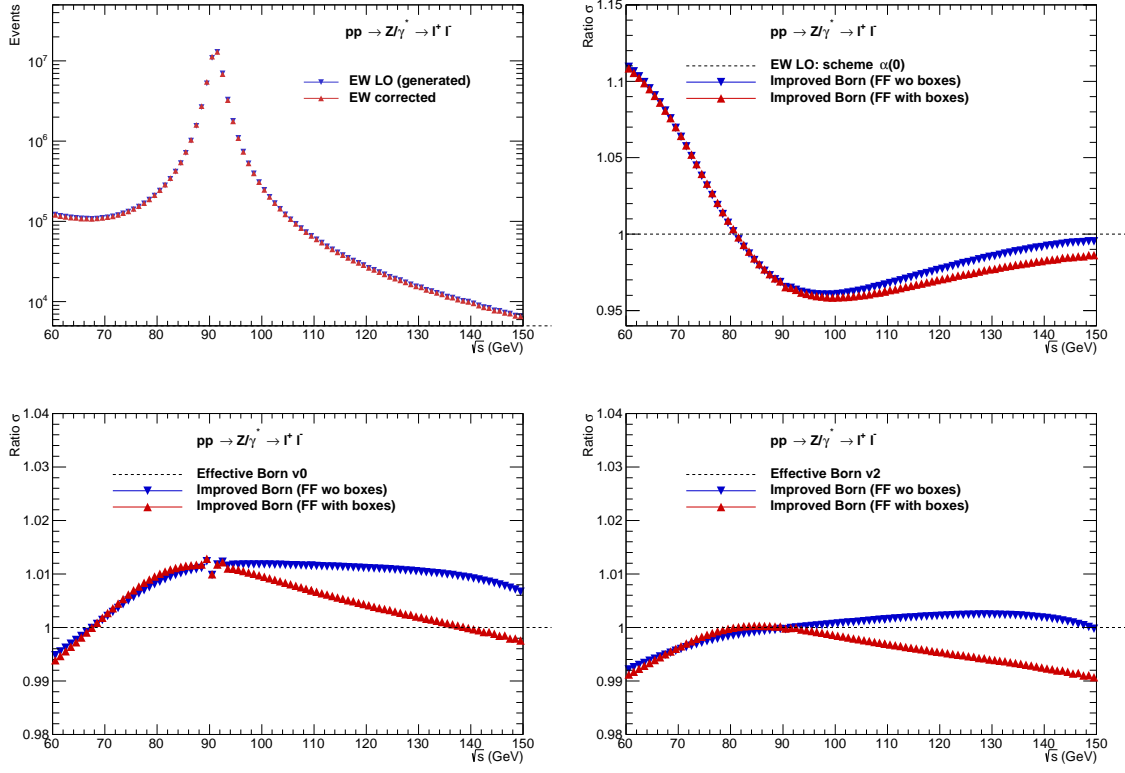


Figure 6: Top-left: Z line-shape distribution as generated with Powheg+MiNLO (blue triangles) and after reweighting introducing all EW corrections discussed (red triangles). The points are barely distinguishable. Ratios of Improved Born results (with and without EW boxes) to Effective Born in: (i) EW LO $\alpha(0)$ scheme are given in top-right, (ii) in bottom-left to Effective Born v_0 and and (iii) in bottom-right plots to Effective Born v_2 .

Table 3: The difference in forward-backward asymmetry, ΔA_{FB} , in the specified mass windows. DIZET 6.45 form-factors and running width was used in re-weighting of LHC $pp \rightarrow Zj$; $Z \rightarrow l^+ l^-$ events simulated at 8 TeV. From the first two lines magnitude of EW corrections with respect to lowest order, $\alpha(0)$ scheme. Following three lines demonstrate precision of Effective Born variants with respect to Improved Born.

Corrections to A_{FB}	$89 < m_{ee} < 93$ GeV	$81 < m_{ee} < 101$ GeV
$A_{FB}(\text{Improved Born, no boxes}) - A_{FB}(\text{EW LO } \alpha(0))$	-0.03491	-0.03515
$A_{FB}(\text{Improved Born, with boxes}) - A_{FB}(\text{EW LO } \alpha(0))$	-0.03489	-0.03514
$A_{FB}(\text{Eff. Born } v_0) - A_{FB}(\text{Improved Born, with boxes})$	-0.00039	-0.00042
$A_{FB}(\text{Eff. Born } v_1) - A_{FB}(\text{Improved Born, with boxes})$	-0.00042	-0.00042
$A_{FB}(\text{Eff. Born } v_2) - A_{FB}(\text{Improved Born, with boxes})$	-0.00022	-0.00024

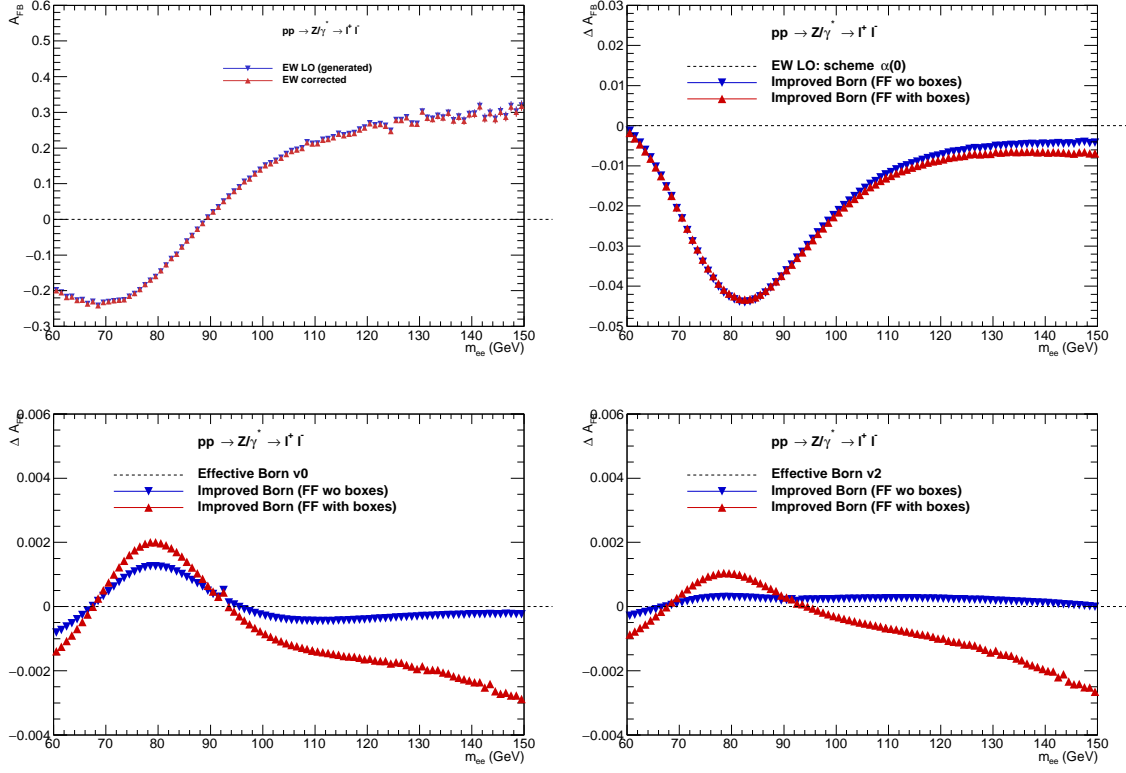


Figure 7: Top-left: the A_{FB} distribution as generated in Powheg+MiNLO sample (blue triangles) and after reweighting introducing all EW corrections (red triangles). The two choices are barely distinguishable. The differences $\Delta A_{FB} = A_{FB} - A_{FB}^{ref}$, of Improved Born results (with and without EW boxes) to Effective Born in: (i) EW LO $\alpha(0)$ scheme are given in top-right, (ii) in bottom-left to Effective Born v0 and and (iii) in bottom-right plots to Effective Born v2.

Table 4: Predictions for different versions of DIZET 6. explained in Appendix A. The Δr , Δr_{em} represent corrections to M_W calculations, see Eq. (7), where $s_W^2 = 1 - \frac{M_W^2}{M_Z^2}$.

Parameter	DIZET 6.21	DIZET 6.42 CPC	DIZET 6.42 (Jeg. 2017)	DIZET 6.45
$\alpha(M_Z^2)$	0.007759954	0.007759954	0.0077549256	0.0077549256
$1/\alpha(M_Z^2)$	128.86674175	128.86674175	128.95030206	128.950302056
M_W (GeV)	80.3560012	80.3535973	80.3621285	80.3589358
Δr	0.03676619	0.03690875	0.03640232	0.03633354
Δr_{rem}	0.01168031	0.01168001	0.01168106	0.01168393
s_W^2	0.22345780	0.22350426	0.22333937	0.22340108
$\sin^2 \theta_W^{eff\ lepton}(M_Z^2)$	0.23173519	0.23174233	0.23157947	0.23149900
$\sin^2 \theta_W^{eff\ up-quark}(M_Z^2)$	0.23162861	0.23174233	0.23147298	0.23139248
$\sin^2 \theta_W^{eff\ down-quark}(M_Z^2)$	0.23150149	0.23174233	0.23134599	0.23126543

5 Electroweak corrections in TauSpinner: library versions and initializations

In the present section we address the impact of the DIZET library variants, which have by now a life-time of more than three decades. The versions of the DIZET EW correction library, which are used in our numerical discussions are presented briefly in Appendix E; details are given in Ref. [18]. Specification of initializations are collected in Appendix A.1. One may wonder if the last version would not suffice. However, availability of the software used for the solutions of legacy measurements is of some value. That is why in Ref. [18] several versions of the present and past EW DIZET library were collected. On the other hand, archived with [14] less popular calculations of the past will not receive our attention.

Each of the four versions of DIZET library of EW effects comes with a wealth of options, which may be activated with their input flags. These options can be used to evaluate the importance of the particular improvement introduced over the years. The graphical programs to monitor the changes are available in TAUOLA/TauSpinner/examples directory. The tau-reweight-test.cxx can be used to demonstrate how events can be corrected with the weight representing improvement from TAUOLA Effective Born of its constant couplings to the one of Improved Born of formula (1) with form-factors interpolated from the text files with tables prepared with KKMC interface to DIZET.

The default for anomalous Born function, introduced for the first time in Ref. [24], is not anymore a dummy but is now the one of EW Improved Born, which uses the EW form-factors tables (if available). The new sub-directory Dizet-example collects programs and scripts for form-factors graphic representation. Plots of form-factors can be drawn, as a function of energy, scattering angle and flavour of incoming partons (it can be an electron-positron pair as well). The integrated over angle partonic cross section σ^{tot} , A_{FB} and P_τ can be graphically presented. Comparison plots can be prepared, either with the help of the FFdrawDwa.C script to compare results with EW form-factors obtained with variants of DIZET initialization, or with FFdraw.C to compare Improved Born and Effective Born of the choice as implemented in TAUOLA package. For technical details see Appendix B. An example results for comparison of Effective Born as encapsulated in TauSpinner/Tauola (version of December 2019) defaults and Improved Born with EW form-factors of DIZET 6.45 were shown in Fig. 3. One should note that differences between semi-analytical results obtained from Improved Born and Effective Born, even in case when detailed tuning of parameters is not performed, are not large from the perspective of many applications.

We concentrate when presenting comparison results on $e^+e^- \rightarrow \tau^+\tau^-$ production process as its phenomenology represents LEP time reference to present day projects, in particular for LHC measurements. Also, parton level cross sections, necessary for LHC phenomenology, are obscured by hadronic interaction effects, thus are more complex for interpretation and require simultaneous evaluation of hadronic interactions.

Numerical results, as in previous section, are monitored with $\sin^2 \theta_W^{eff}$, P_τ , A_{FB} and parton level σ^{tot} . In Fig. 8 and Table 4 it is shown how results depend on the library version. The presentation in Table 4 includes predictions on $\alpha(M_Z^2)$, M_W , Δr , and $\sin^2 \theta_W^{eff}$. Further results are delegated to Appendices.

By inspection of Table 4 one can conclude that the choice of EW library variant is not of great importance, unless precision better than $20 \cdot 10^{-5}$ on $\sin^2 \theta_W^{eff}$ is required. Even if precision requirements are not very demanding one should keep in mind that below 40 GeV in older versions of DIZET the hadronic part of $\Pi_W(s)$ was set to zero. See also Fig. 3 for minor discontinuity at 30 GeV due to edge of tabulation zones. Further details on the impact of change of options/flags of DIZET 6.45 are collected in Tables 8, 9 of Appendix A.2.

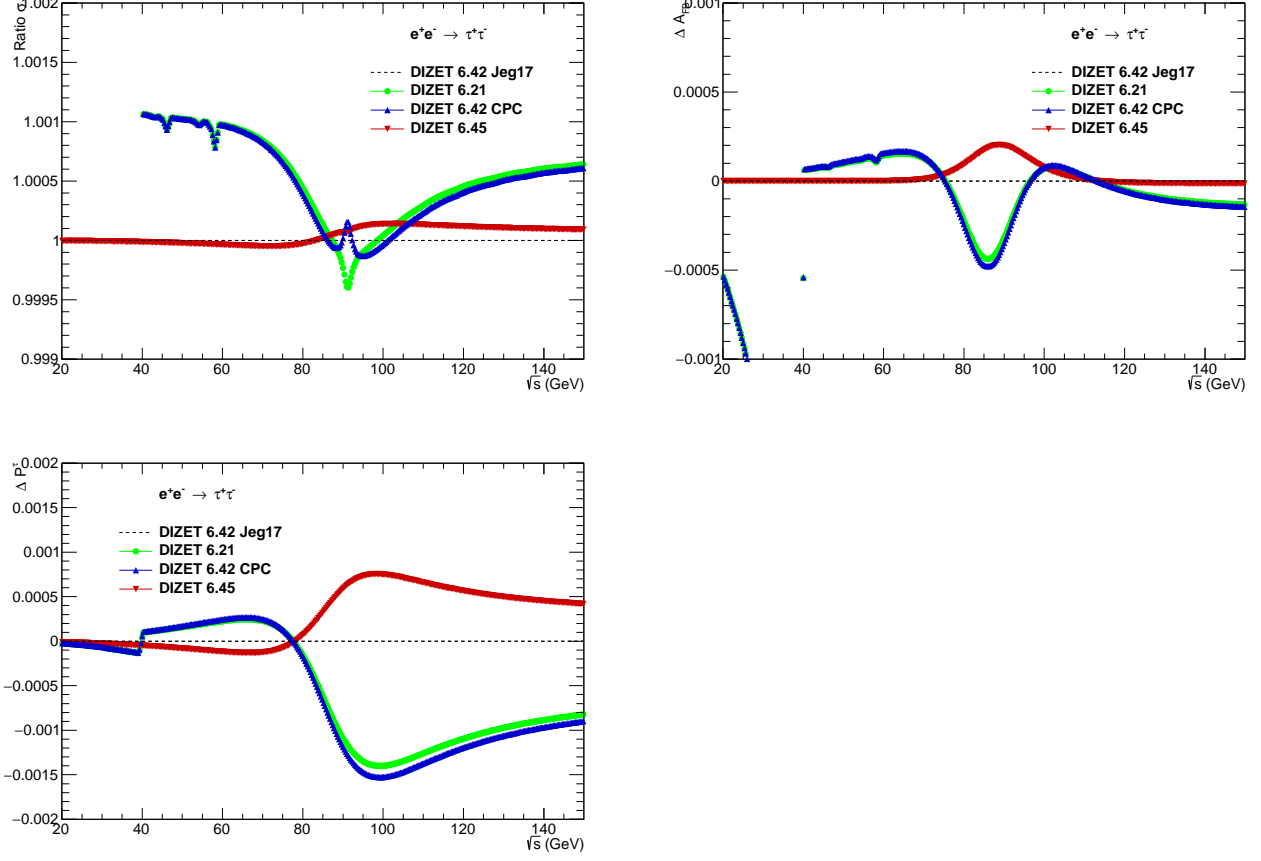


Figure 8: Comparison of $\sigma_{Tot}(m_{\tau^+\tau^-})$, $A_{FB}(m_{\tau^+\tau^-})$ and $P_\tau(m_{\tau^+\tau^-})$, obtained from TauSpinner calculations of Improved Born and EW tables calculated with the DIZET libraries. As a reference, version 6.42 improved with photon vacuum polarization of Ref. [25] is used. Note, that interface of photon vacuum polarization of DIZET 6.42 and 6.21 prevented its calculation below 40 GeV. This, and other minor parameter variation in particular of M_Z and Γ_Z , lead to bumps on the plots which do not need to be investigated now, and even for the precision tests of the SM at LHC, as they are smaller than precision requirements. On the other hand, proper adjustment for the effects important at (and around) the Z peak need to be performed. The corresponding EW-corrected M_W , $\sin^2 \theta_W^{eff}$ and α at the Z pole are collected in Table 4. Similar results can be obtained from TauSpinner for the quark level Effective Born and Improved Born predictions.

5.1 Parametric uncertainties

The precision of the EW calculations depends not only on the EW scheme used for the calculations (see e.g. [26, 27], but also on imposed set of input parameters and corresponding parametric uncertainties. Parametric uncertainties are defined as the ones due to ambiguities of EW calculation inputs, such as m_t , M_W or $\Delta\alpha_h^{(5)}(s)$. That is the reason why precision of these input parameters (taken from measurements), specially M_W or $\sigma_{e^+e^- \rightarrow \text{hadrons}}^{tot}(s)$ (for $\alpha_{QED}(M_Z^2)$), is of importance. For clarity of the presentation this topic is covered only in Appendices A.2, A.3, in particular in Tables 8, 9, 10, 11. We show how some phenomenologically sound quantities depend on initialization ambiguities for $\alpha(0)$ EW scheme used in the DIZET library. In particular how do they depend on: (i) distinct $\Delta\alpha_h^{(5)}(s)$ parametrization, (ii) uncertainty from changing $\Delta\alpha_h^{(5)}(M_Z^2)$ by ± 0.0001 , (iii) uncertainty due to top mass change by ± 0.5 GeV. The estimated total parametric uncertainty for EW $\alpha(0)$ scheme used for $\sin^2 \theta_W^{eff}(M_Z^2)$ is about 0.00005.

To summarize, these example results can be useful by themselves but they represent a precondition for the choice of the EW schemes and their inputs. Large parametric uncertainties could indicate that some schemes are not optimal. That is why they contribute to evaluation of reliability for the Effective Born (effective couplings) concept, too.

6 Summary

One loop EW corrections play important role in the precision tests of the Standard Model. At the same time, other effects, related to special classes of higher order corrections had to be taken into account. That is the reason, why special libraries of EW corrections were developed, maintained and gradually improved. Over the last 30 years the DIZET library was established as a prominent one. Special role was played by the so-called EW $\alpha(0)$ scheme. This scheme and DIZET library found large spectrum of applications, not only in phenomenology of LEP e^+e^- collisions but $p\bar{p}$ and pp Tevatron and LHC experiments as well. An attempt to archive distinct versions of EW libraries is provided in [18]. These results and methods need to be reproducible at the time of future FCC or similar experiments. Negligible differences of the past may play important role for future higher precision projects. From our investigations, see Subsection 4.1, 4.2, we can conclude that effective couplings approach can be useful for $\sin^2 \theta_W^{eff}$ precision up to about $20 \cdot 10^{-5}$. Beyond that, Improved Born without simplifications is needed.

In principle, DIZET relies on one-loop calculations, but it is supplemented with dominant higher order terms. Presented implementation of TauSpinner weights enable discussion of particular classes of higher order effects. In the present paper we have explained how the numerical impact of some effects of EW results can be imprinted into broad spectrum of simulation samples where EW loop effects are missing, or impact of their initialization is to be studied. We have installed useful for that purpose algorithms into TauSpinner library. Example numerical results are focused on center-of-mass system energy dependence of total cross sections, forward-backward asymmetry of leptons, and τ lepton polarization. Those were studied for e^+e^- and pp collisions.

New TauSpinner algorithms have potential to improve e.g. EW effects in simulation samples obtained from programs predominantly of strong interactions. We have shown results of re-weighting with different levels of sophistication for implementation of EW corrections. Let us point out that from the perspective of forthcoming efforts on higher-order high precision EW calculations, TauSpinner/DIZET algorithms may be used as a set of methods for evaluation which contributions (and to which order) need to be taken into account to attain requested precision level.

Acknowledgments

E.R-W. would like to thank Daniel Froidevaux and colleagues from ATLAS Collaboration Standard Model Working Group for numerous inspiring discussions on the applications of presented here implementation of EW corrections to the $\sin^2 \theta_W^{eff}$ measurement at LHC.

References

- [1] ALEPH, CDF, D0, DELPHI, L3, OPAL, SLD, LEP Electroweak Working Group, Tevatron Electroweak Working Group, SLD Electroweak, Heavy Flavour Groups Collaboration, 1012.2367.
- [2] SLD Electroweak Group, DELPHI, ALEPH, SLD, SLD Heavy Flavour Group, OPAL, LEP Electroweak Working Group, L3 Collaboration, S. Schael *et al.*, *Phys. Rept.* **427** (2006) 257–454, hep-ex/0509008.
- [3] M. Davier, L. DufLOT, F. Le Diberder, and A. Rouge, *Phys. Lett. B* **306** (1993) 411–417.
- [4] P. Gambino and A. Sirlin, *Phys. Rev. D* **49** (1994) 1160–1162, hep-ph/9309326.
- [5] D. Yu. Bardin, P. Christova, M. Jack, L. Kalinovskaya, A. Olchevski, S. Riemann, and T. Riemann, *Comput. Phys. Commun.* **133** (2001) 229–395, hep-ph/9908433.

- [6] A. Barroso *et al.*, “ELECTROWEAK RADIATIVE CORRECTIONS AT LEP ENERGIES”, in *ECFA Workshop: LEP 200*, 4, 1987.
- [7] D. Y. Bardin, M. Grunewald, and G. Passarino, hep-ph/9902452.
- [8] W. Hollik, U. Meier, and S. Uccirati, *Nucl. Phys. B* **731** (2005) 213–224, hep-ph/0507158.
- [9] E. Richter-Was and Z. Was, *Eur. Phys. J.* **C76** (2016), no. 8 473, 1605.05450.
- [10] E. Richter-Was and Z. Was, *Eur. Phys. J.* **C77** (2017), no. 2 111, 1609.02536.
- [11] Z. Czyżczula, T. Przedzinski, and Z. Was, *Eur.Phys.J.* **C72** (2012) 1988, 1201.0117.
- [12] T. Przedzinski, E. Richter-Was, and Z. Was, 1802.05459.
- [13] E. Richter-Was and Z. Was, *Eur. Phys. J.* **C79** (2019), no. 6 480, 1808.08616.
- [14] S. Jadach, B. F. L. Ward, and Z. Was, *Comput. Phys. Commun.* **79** (1994) 503.
- [15] S. Jadach, Z. Was, and B. F. L. Ward, *Comput. Phys. Commun.* **130** (2000) 260, Up to date source available from <http://home.cern.ch/jadach/>.
- [16] S. Jadach, B. Ward, and Z. Was, *Phys. Rev. D* **63** (2001) 113009, hep-ph/0006359.
- [17] D. Yu. Bardin, M. S. Bilenky, T. Riemann, M. Sachwitz, and H. Vogt, *Comput. Phys. Commun.* **59** (1990) 303–312.
- [18] A. Arbuzov, S. Jadach, Z. Was, B. F. L. Ward, and S. A. Yost, The Monte Carlo Program KKMC, for the Lepton or Quark Pair Production at LEP/SLC Energies – updated of electroweak calculations, IFJPAN-IV-2020-05 BU-HEPP-2020-01.
- [19] R. Kleiss and W. J. Stirling, *Nucl. Phys.* **B262** (1985) 235.
- [20] F. A. Berends, R. Kleiss, and S. Jadach, *Comput. Phys. Commun.* **29** (1983) 185–200.
- [21] E. Mirkes and J. Ohnemus, *Phys. Rev.* **D51** (1995) 4891–4904, hep-ph/9412289.
- [22] J. C. Collins and D. E. Soper, *Phys. Rev.* **D16** (1977) 2219.
- [23] S. Banerjee and Z. Was, *CERN Yellow Reports: Monographs* **3** (2020) 211–212.
- [24] S. Banerjee, J. Kalinowski, W. Kotlarski, T. Przedzinski, and Z. Was, *Eur.Phys.J.* **C73** (2013) 2313, 1212.2873.
- [25] F. Jegerlehner, “ $\alpha_{QED,eff}(s)$ for precision physics at the FCC-ee/ILC”, in *Theory report on the 11th FCC-ee workshop*, pp. 9–37, 2019.
- [26] S. Alioli *et al.*, *Eur. Phys. J.* **C77** (2017), no. 5 280, 1606.02330.
- [27] S. Dittmaier, A. Huss, and C. Schwinn, *Nucl. Phys.* **B885** (2014) 318–372, 1403.3216.
- [28] D. Yu. Bardin, P. K. Khristova, and O. M. Fedorenko, *Nucl. Phys.* **B175** (1980) 435–461.
- [29] D. Yu. Bardin, P. K. Khristova, and O. M. Fedorenko, *Nucl. Phys.* **B197** (1982) 1–44.
- [30] A. Sirlin, *Phys. Rev.* **D22** (1980) 971–981.
- [31] F. Jegerlehner, *EPJ Web Conf.* **218** (2019) 01003, 1711.06089.
- [32] A. B. Arbuzov, M. Awramik, M. Czakon, A. Freitas, M. W. Grunewald, K. Monig, S. Riemann, and T. Riemann, *Comput. Phys. Commun.* **174** (2006) 728–758, hep-ph/0507146.
- [33] S. Eidelman and F. Jegerlehner, *Z. Phys.* **C67** (1995) 585–602, hep-ph/9502298.
- [34] G. Degrassi, S. Fanchiotti, F. Feruglio, P. Gambino, and A. Vicini, *Phys. Lett.* **B350** (1995) 75–84, hep-ph/9412380.
- [35] G. Degrassi, F. Feruglio, A. Vicini, S. Fanchiotti, and P. Gambino, “Two loop corrections for electroweak processes”, in *’95 electroweak interactions, unified theories. Proceedings, Leptonic Session of the 30th Rencontres de Moriond, Moriond Particle Physics Meetings, Les Arcs, France, March 11-18, 1995*, pp. 77–85, 1995, hep-ph/9507286.
- [36] G. Degrassi, P. Gambino, and A. Vicini, *Phys. Lett.* **B383** (1996) 219–226, hep-ph/9603374.

- [37] G. Degrandi and P. Gambino, *Nucl. Phys.* **B567** (2000) 3–31, hep-ph/9905472.
- [38] A. Freitas, W. Hollik, W. Walter, and G. Weiglein, *Phys. Lett.* **B495** (2000) 338–346, [Erratum: *Phys. Lett.* **B570**, no. 3–4, 265 (2003)], hep-ph/0007091.
- [39] A. Freitas, S. Heinemeyer, W. Hollik, W. Walter, and G. Weiglein, *Nucl. Phys. Proc. Suppl.* **89** (2000) 82–87, hep-ph/0007129.
- [40] A. Freitas, W. Hollik, W. Walter, and G. Weiglein, *Nucl. Phys.* **B632** (2002) 189–218, [Erratum: *Nucl. Phys.* **B666**, 305 (2003)], hep-ph/0202131.
- [41] M. Awramik, M. Czakon, A. Freitas, and G. Weiglein, *Phys. Rev.* **D69** (2004) 053006, hep-ph/0311148.
- [42] M. Awramik, M. Czakon, A. Freitas, and G. Weiglein, *Phys. Rev. Lett.* **93** (2004) 201805, hep-ph/0407317.
- [43] M. Awramik, M. Czakon, and A. Freitas, *JHEP* **11** (2006) 048, hep-ph/0608099.
- [44] I. Dubovyk, A. Freitas, J. Gluza, T. Riemann, and J. Usovitsch, *Phys. Lett.* **B762** (2016) 184–189, 1607.08375.
- [45] I. Dubovyk, A. Freitas, J. Gluza, T. Riemann, and J. Usovitsch, *JHEP* **08** (2019) 113, 1906.08815.
- [46] L. Avdeev, J. Fleischer, S. Mikhailov, and O. Tarasov, *Phys. Lett.* **B336** (1994) 560–566, [Erratum: *Phys. Lett.* **B349**, 597 (1995)], hep-ph/9406363.
- [47] Particle Data Group Collaboration, M. Tanabashi *et al.*, *Phys. Rev.* **D98** (2018), no. 3 030001.
- [48] ATLAS Collaboration, M. Aaboud *et al.*, *Phys. Lett.* **B784** (2018) 345–366, 1806.00242.
- [49] ATLAS Collaboration, M. Aaboud *et al.*, *Eur. Phys. J.* **C78** (2018), no. 2 110, [Erratum: *Eur. Phys. J.* **C78**, no. 11, 898 (2018)], 1701.07240.
- [50] ATLAS Collaboration, M. Aaboud *et al.*, *Eur. Phys. J.* **C79** (2019), no. 4 290, 1810.01772.
- [51] LHC EW WG, “<https://lpc.web.cern.ch/electroweak-precision-measurements-lhc-wg>”, 2018–2020.
- [52] A. Blondel, J. Gluza, S. Jadach, P. Janot, and T. Riemann, eds., *Theory for the FCC-ee: Report on the 11th FCC-ee Workshop Theory and Experiments*, vol. 3/2020 of *CERN Yellow Reports: Monographs*, Geneva, CERN, 5, 2019.
- [53] N. Davidson, G. Nanava, T. Przedzinski, E. Richter-Was, and Z. Was, TAUOLA and TAUOLA C++ Interface source code and documentation available from <http://wasm.web.cern.ch/wasm/C++.html> or <http://tauolapp.web.cern.ch>.
- [54] N. Davidson, G. Nanava, T. Przedzinski, E. Richter-Was, and Z. Was, *Comput. Phys. Commun.* **183** (2012) 821–843, 1002.0543.
- [55] D. Bardin, A. Leike, T. Riemann, and M. Sachwitz, *Phys. Lett. B* **206** (1988) 539–542.
- [56] A. Arbuzov, S. Jadach, Z. Was, B. Ward, and S. Yost, *Comput. Phys. Commun.* **260** (2021) 107734, 2007.07964.
- [57] S. Jadach, B. F. L. Ward, and Z. Was, *Phys. Rev.* **D88** (2013), no. 11 114022, 1307.4037.

A DIZET EW corrections

The DIZET package relies on *on-mass-shell* (OMS) normalization scheme [28, 29], thus the $(G_\mu, \alpha(0), M_Z)$ are the principal input parameters, dependence on m_h , top quark and lepton masses are numerically less important. The OMS normalization scheme input includes masses of all fundamental particles, both fermions and bosons, electromagnetic coupling constant $\alpha(0)$ and strong coupling $\alpha_s(M_Z)$. The OMS is used with modifications. The dependence on the ill-defined masses of the light quarks u, d, c, s and b is solved by dispersion relation, for details see [5]. Another exception is W -boson mass M_W , which still can be predicted with better theoretical uncertainties than experimentally measured values, exploiting the very precise knowledge of the Fermi constant in μ -decay G_μ . The discussed above EW scheme is in the literature often called EW $\alpha(0)$ scheme [2]. The M_W is calculated iteratively from the equation

$$M_W = \frac{M_Z}{\sqrt{2}} \sqrt{1 + \sqrt{1 - \frac{4A_0^2}{M_Z^2(1 - \Delta r)}}}, \quad (5)$$

where

$$A_0 = \sqrt{\frac{\pi\alpha(0)}{\sqrt{2}G_\mu}}. \quad (6)$$

The Sirlin's parameter Δr [30]

$$\Delta r = \Delta\alpha(M_Z) + -\Delta r_L + \Delta r_{em} \quad (7)$$

is also calculated iteratively, and the definition of $\Delta r_L, \Delta r_{em}$ involve resummation and higher order corrections. Since this term implicitly depends on M_W and M_Z iterative procedure is needed. The resummation term in formula (7) is not formally justified by renormalisation group arguments, correct generalization is to compute higher order corrections, see more discussion in [5]. The electromagnetic coupling evolves from Thomson limit and for Z -boson energy scale receives corrections

$$\Delta\alpha(M_Z) = \Delta\alpha_h^{(5)}(M_Z) + \Delta\alpha_l(M_Z) + \Delta\alpha_t(M_Z) + \Delta\alpha^{\alpha\alpha_s}(M_Z) \quad (8)$$

The hadronic vacuum polarization correction is contained in the quantity denoted as $\Delta\alpha_h^{(5)}(M_Z)$, which is treated as one of the input parameters. It can be either computed from quark masses or, preferably, fitted to experimental low energy $e^+e^- \rightarrow \text{hadrons}$ data [31]. The leptonic loop correction $\Delta\alpha_l(M_Z)$ is calculated analytically. Both $\Delta\alpha_h^{(5)}(M_Z)$ and $\Delta\alpha_l(M_Z)$ are significant, respectively about 0.0275762 and 0.0314976, the remaining terms are rather marginal, respectively about $-5 \cdot 10^{-5}$ and $-1 \cdot 10^{-5}$.

In the OMS renormalisation scheme the weak mixing angle is defined uniquely through the gauge-boson masses:

$$\sin^2\theta_W = s_W^2 = 1 - \frac{M_W^2}{M_Z^2}. \quad (9)$$

With this scheme, measuring $\sin^2\theta_W$ would be equivalent to indirect measurement of M_W^2 through the relation (9).

A.1 Initialization flags and input parameters

The recommended sets of flags are quite stable since 1995, new options consider updated parametrisations of the vacuum polarization hadronic corrections $\Delta\alpha_{had}^{(5)}$ (flag IHVP), updated calculations for two loop fermionic corrections (flag IAMT4) and updated three-loop corrections (flag IAFMT).

In Table 5 we collected information on the initialization flags recommended for different versions of DIZET 6.XX. For detailed information about meaning of the individual flags see DIZET 6.XX documentations [17, 5, 32].

Let us here just explain those, for which recommended values have changed since version DIZET 6.21:

- Switch for Hadronic vacuum polarization corrections $\Delta\alpha_{had}^{(5)}$:
IHVP = 1 parametrization of [33]
IHVP = 5 parametrization of [31]
- Switch for resummation of the leading $O(G_f m_t^2)$ EW corrections:
IAMT4 = 4 with two-loop sub-leading corrections and resummation [34, 35, 36, 37]
IAMT4 = 5 with fermionic two-loop corrections to M_W [38, 39, 40]
IAMT4 = 6 with complete two-loop corrections to M_W [41] and fermionic two-loop corrections to $\sin^2\theta_W^{eff\ lep}$ [42]
IAMT4 = 7 with complete two-loop corrections to $\sin^2\theta_W^{eff\ lep}$ and $\sin^2\theta_W^{eff\ lb}$ [43, 44]
IAMT4 = 8 with complete two-loop corrections to $\sin^2\theta_W^{eff}$ [45]
- Switch for three-loop corrections $O(\alpha_s^2)$ to the EW ρ parameter:
IAFMT = 1 corrections $O(G_\mu m_t^2 \alpha_s^2)$ included [46]
IAFMT = 2 corrections $O(G_\mu m_t^2 \alpha_s^2)$, $O(G_\mu M_Z^2 \alpha_s^2 + \log(m_t^2))$ included IAFMT = 3 corrections $O(G_\mu m_t^2 \alpha_s^2)$, $O(G_\mu M_Z^2 \alpha_s^2 + \log(m_t^2))$ and $O(G_\mu M_Z^2 / m_t^2 \alpha_s^2)$ included

Since LEP time physics measurements evolved, and as a consequence initialization parameters as well. For the recent status summary see last edition by Particle Data Group [47]. The Higgs boson has been discovered at LHC and its mass measured with precision of 25 MeV [48]. The W boson mass is known at LHC with precision better than 18 MeV [49] and the top mass is known with precision much better than 1 GeV [50].

In Tables 6 and 7 we collected initialization parameters: masses and couplings, used of the paper numerical evaluation. The exact values of some of them, which serve as benchmark values for different comparisons, has been chosen as such to be fully compatible with the ongoing studies of the LHC EW Working Group [51].

Table 5: DIZET initialization flags: different versions defaults.

Input NPAR()	Internal flag	DIZET 6.21 Defaults in [17]	DIZET 6.42 Defaults in [32]	DIZET 6.45	Comments
NPAR(1)	IHVP	1	1	5	$\Delta\alpha_{had}^{(5)}$ param. from [31] in v6.45 New development in v6.42, v6.45
NPAR(2)	IAMT4	4	4	8	
NPAR(3)	IQCD	3	3	3	M_W calculated with formula (5)
NPAR(4)	IMOMS	1	1	1	
NPAR(5)	IMASS	0	0	0	
NPAR(6)	ISCRE	0	0	0	
NPAR(7)	IALEM	3	3	3	
NPAR(8)	IMASK	0	0	0	Not used since v6.21
NPAR(9)	ISCAL	0	0	0	
NPAR(10)	IBARB	2	2	2	
NPAR(11)	IFTJR	1	1	1	
NPAR(12)	IFACR	0	0	0	
NPAR(13)	IFACT	0	0	0	
NPAR(14)	IHIGS	0	0	0	
NPAR(15)	IAMFT	1	3	3	
NPAR(16)	IEWLC	1	1	1	
NPAR(17)	ICZAK	1	1	1	
NPAR(18)	IHIG2	1	1	1	
NPAR(19)	IALE2	3	3	3	
NPAR(20)	IGREF	2	2	2	
NPAR(21)	IDDZZ	1	1	1	
NPAR(22)	IAMW2	0	0	0	
NPAR(23)	ISFSR	1	1	1	
NPAR(24)	IDMWW	0	0	0	
NPAR(25)	IDSWW	0	0	0	

Table 6: The EW parameters used at tree-level EW, with on-mass-shell definition (LEP convention).

Parameter	$(\alpha(0), G_\mu, M_Z)$
M_Z (GeV)	91.1876
Γ_Z (GeV)	2.4952
Γ_W (GeV)	2.085
$1/\alpha$	137.035999139
α	0.007297353
G_μ (GeV ⁻²)	$1.1663787 \cdot 10^{-5}$
M_W (GeV)	80.93886
s_W^2	0.2121517
$\alpha_s(M_Z)$	0.12017890

Table 7: Values of fermions and Higgs boson masses used for calculating EW corrections.

Parameter	Mass (GeV)	Description
m_e	5.1099907e-4	mass of electron
m_μ	0.1056583	mass of muon
m_τ	1.7770500	mass of tau
m_u	0.0620000	mass of up-quark
m_d	0.0830000	mass of down-quark
m_c	1.5000000	mass of charm-quark
m_s	0.2150000	mass of strange-quark
m_b	4.7000000	mass of bottom-quark
m_t	173.0	mass of top quark
m_H	125.0	mass of Higgs boson

A.2 Numerical results

The `DIZET` library, when invoked, provide tabulated s, t -dependent form-factors. It calculates also M_W , Stirling parameter $\Delta r, \Delta r_{em}$ and flavour-dependent $\sin^2 \theta_W^{eff}$ at Z peak. In Table 4 we have collected numerical results on predicted masses and couplings, including EW corrections. Those values come directly as control printout from `DIZET 6.XX` code. In total, evolution of the implemented EW corrections, lead to shift in the predicted M_W by +3 MeV, on-shell s_W^2 by -0.00005 and $\sin^2 \theta_W^{eff lepton}$ by -0.00020. Let us comment on this evolution:

- The change in $\alpha(M_Z^2)$ is due to improvements in the theoretical predictions and experimental low-energy measurements over last 25 years, and following update in the used parametrization from [33] to [31].
- The Δr and Δr_{rem} , which are displayed separately, represent gauge invariant corrections to M_W calculation as shown in formulas (5) and (7). The Δr is affected by options used for calculating Δr_L , which depends on the flag `AMT4` used. It also depends on the parametrization of $\Delta \alpha(M_Z)$. The sensitivity of the Δr_{rem} to all changed introduced between `v6.21` and `v6.45` is almost negligible.
- As a consequence of different predicted M_W , the on-shell s_W^2 has evolved as well.
- Evolution of $\sin^2 \theta_W^{eff f}$, illustrated with Fig. 2, comes from changing s_W^2 and $\mathcal{K}^f(s, t)$ form-factors. It impact $P^\tau, A_{FB}, \sigma^{tot}$ too.

In Table 8, we document impact of changing only parametrization of $\Delta \alpha_{had}^{(5)}(s)$, with other parameters and flags unchanged. Dominant effect comes from EW corrections to M_W , which shifts its value by +8.4 MeV, reflected in change of s_W^2 by -0.00016. The impact on the form-factors is less significant and final shift in the $\sin^2 \theta_W^{eff lepton}(M_Z^2)$ is of -0.00023.

In Table 9, we document impact of changing only two-loop corrections to M_W , with other parameters and flags unchanged. The resulting shift on M_W is smaller, -2.9 MeV only, resulting in +0.00006 shift on s_W^2 and, while multiplied with form-factors which also have changed, correspondingly in -0.00008 shift on $\sin^2 \theta_W^{eff lepton}(M_Z^2)$.

A.3 Parametric uncertainties on $\sin^2 \theta_W^{eff}(M_Z^2)$ predictions

We have studied dominant parametric uncertainties from $\Delta \alpha_h^{(5)}(M_Z^2)$ and m_t for $\sin^2 \theta_W^{eff}(M_Z^2)$ prediction. Recent detailed discussion on the parametric uncertainties of SM parameters can be found in [52]. Both components of $\sin^2 \theta_W^{eff}(M_Z^2) = \text{Re} \mathcal{K}^f(M_Z^2, -\frac{M_Z^2}{2}) \cdot s_W^2$ definition are sensitive to parametric uncertainties.

- In Table 10 we show impact of changing $\Delta \alpha_h^{(5)}(M_Z^2) \pm 0.0001$, which is the uncertainty of the parametrization of [31]. The resulting uncertainty on $\sin^2 \theta_W^{eff}(M_Z^2)$ is of ± 0.000035 .
- In Table 11 we show impact of changing $m_t \pm 0.5$ GeV, which is roughly the anticipated uncertainty of the measurements at LHC [50]. The resulting uncertainty on $\sin^2 \theta_W^{eff}(M_Z^2)$ is of ± 0.000016 .

The total parametric uncertainty, added in quadrature, on $\sin^2 \theta_W^{eff}(M_Z^2)$ is about ± 0.00005 .

B Technical documentation of upgrades for TAUSPINNER electroweak re-weighting code

In `TauSpinner` the Improved Born of (1) is coded as default for its `nonSMBorn` function. If form-factors are available, look-up tables present, then they will be used for re-weighting algorithm. At default, it will be then assumed⁷ that sample was generated with Effective Born `Tauola/LEP` variant, see Table 1. A wealth of options is available for EW form-factors calculation, see Section A.1, Table 5 and Section E. Choice of options simplifying Improved Born to the cases closer, or to effective Born itself, are listed in Table 13.

To monitor in a quick manner look-up tables with form-factors, root scripts `FFdraw.C` and `FFdrawDwa.C` are provided, see Appendix 5. These scripts provide semi-analytical results for Born-level cross section, A_{FB} and A_{pol} as a function of centre-of-mass energy, for incoming e^+e^- (or $u\bar{u}, d\bar{d}$) pairs. Two versions can be compared; e.g. EW improved Born with default Effective `Tauola/LEP` Born of `TauSpinner`, or of two variants of EW-initialization.

In the distribution tar-ball [53] of `Tauola/TauSpinner` there are two example main programs, which demonstrate how re-weighting of EW effects is implemented (on the `LHE` and `HepMC` event formats) and how analytically these effects can be

⁷If it is not the case, the weight will not be appropriate if `TauSpinner` initialization is not adjusted.

Table 8: The DIZET 6.45 predictions for two different parametrisations of $\Delta\alpha_h^{(5)}(M_Z^2)$. Other flags as in Table 5.

Parameter	$\Delta\alpha_h^{(5)}(M_Z^2) = 0.0280398$ (param. Jegerlehner 1995)	$\Delta\alpha_h^{(5)}(M_Z^2) = 0.0275762$ (param. Jegerlehner 2017)	Δ
$\alpha(M_Z^2)$	0.0077587482	0.0077549256	
$1/\alpha(M_Z^2)$	128.88676996	128.95030224	
M_W (GeV)	80.350538	80.358936	+8.4 MeV
Δr	0.03690873	0.03640338	
Δr_{rem}	0.01168001	0.01167960	
s_W^2	0.22356339	0.22340108	- 0.00016
$\sin^2\theta_W^{eff\ lepton}(M_Z^2)$	0.23166087	0.23149900	- 0.00023
$\sin^2\theta_W^{eff\ up-quark}(M_Z^2)$	0.23155425	0.23139248	- 0.00016
$\sin^2\theta_W^{eff\ down-quark}(M_Z^2)$	0.23142705	0.23126543	- 0.00016

Table 9: The DIZET 6.45 predictions with improved treatment of two-loop corrections. Other flags as in Table 5.

Parameter	AMT4= 4	AMT4= 8	Δ
$\alpha(M_Z^2)$	0.0077549256113	0.0077549256002	
$1/\alpha(M_Z^2)$	128.95030206	128.95030224	
M_W (GeV)	80.361846	80.358936	- 2.9 MeV
Δr	0.03640338	0.03640338	
Δr_{rem}	0.01167960	0.01167960	
s_W^2	0.22333971	0.22340108	+ 0.00006
$\sin^2\theta_W^{eff\ lepton}(M_Z^2)$	0.23157938	0.23149900	-0.00008
$\sin^2\theta_W^{eff\ up-quark}(M_Z^2)$	0.23147290	0.23139248	-0.00008
$\sin^2\theta_W^{eff\ down-quark}(M_Z^2)$	0.23134590	0.23126543	-0.00008

Table 10: The DIZET 6.45 predictions: uncertainty from changing $\Delta\alpha_h^{(5)}(M_Z^2) = 0.0275762$ (param. [31]), by ± 0.0001 .

Parameter	$\Delta\alpha_h^{(5)}(M_Z^2) - 0.0001$	$\Delta\alpha_h^{(5)}(M_Z^2) = 0.0275762$	$\Delta\alpha_h^{(5)}(M_Z^2) + 0.0001$	$\Delta/2$
$\alpha(M_Z^2)$	0.0077541016	0.0077549256	0.0077557498	
$1/\alpha(M_Z^2)$	128.96400565	128.95030224	128.93659846	
M_W (GeV)	80.360747	80.358936	80.357124	1.8 MeV
Δr	0.03629414	0.03640338	0.03651261	
Δr_{rem}	0.01167983	0.01167960	0.01167938	
s_W^2	0.22336607	0.22340108	0.22343610	0.000035
$\sin^2\theta_W^{eff\ lepton}(M_Z^2)$	0.23146409	0.23149900	0.23153392	0.000035
$\sin^2\theta_W^{eff\ up-quark}(M_Z^2)$	0.23135758	0.23139248	0.23142737	0.000035
$\sin^2\theta_W^{eff\ down-quark}(M_Z^2)$	0.23123057	0.23126543	0.23130029	0.000035

Table 11: The DIZET 6.45 predictions: uncertainty from changing top-quark mass $m_t = 173.0$ GeV by ± 0.5 GeV.

Parameter	$m_t - 0.5$ GeV	$m_t = 173.0$ GeV	$m_t + 0.5$ GeV	$\Delta/2$
$\alpha(M_Z^2)$	0.0077549221	0.0077549256	0.0077549291	
$1/\alpha(M_Z^2)$	128.95036003	128.95030224	128.95024461	
M_W (GeV)	80.355935	80.358936	80.361941	3 MeV
Δr	0.03658500	0.03640338	0.03622132	
Δr_{rem}	0.01167011	0.01167960	0.01168907	
s_W^2	0.22345908	0.22340108	0.22334300	0.000058
$\sin^2\theta_W^{eff\ lepton}(M_Z^2)$	0.23151389	0.23149900	0.23148410	0.000016
$\sin^2\theta_W^{eff\ up-quark}(M_Z^2)$	0.23140736	0.23139248	0.23137758	0.000016
$\sin^2\theta_W^{eff\ down-quark}(M_Z^2)$	0.23128031	0.23126543	0.23125053	0.000016

Table 12: EW form-factors of formula (1) calculated by DIZET and provided by KKMC tabulation code. Names as used in: formula (1), KKMC tabulation code and in Dizet-example are collected. In Effective Born Eq. (4) numerical constants replace form-factors of Improved Born (1). Depending on Effective Born version (see Table 1) $\sin^2 \theta_W$ of Improved Born is replaced by $\sin^2 \theta_W^{eff}$ or by flavour-dependent variants $\sin^2 \theta_W^{eff\,l/up/down}$, the $\rho_{ef}(s,t)$ is then replaced with constant ρ_{ef} . Similarly $\alpha(0)$ is replaced with $\alpha(M_Z)$

Form-factor	in KKMC	in Dizet example	in Effective Born
$\rho_{ef}(s,t)$	GSW (1)	FF1	1
v1			1.005
v2			1.005403 (up) 1.005889 (down)
$K_e(s,t)$	GSW (2)	FF2	1
$K_f(s,t)$	GSW (3)	FF3	1
$K_{ef}(s,t)$	GSW (4)	FF4	1
--	--	--	-
$\Pi_\gamma(s)$	GSW (6)	FF6	1

monitored. These programs, respectively `tau-reweight-test.cxx` and `Dizet-example/table-parsing-test.cxx` need explanation because they evolved with time and more initialization options were introduced. In particular, to evaluate numerical differences between Effective Born and EW Improved Born as well as of the intermediate variants; the steering flag for the variants is `keyGSW`. Note, that to re-weight, program needs to flip for each event, initialization between two variants and save some intermediate results to avoid massive recalculations. The semi-analytical `table-parsing-test.cxx` is obviously much faster. It is useful for study of small effects and not only to checks of the correctness for EW form-factors tabulation.

Let us collect technical details for these programs and dependencies between routines:

- `Dizet-example/table-parsing-test.cxx`. This semi-analytic program is fast, does not require continuous inter-changing between variants of initialization and is suitable to study small variation for predictions due to initialization fine tuning. It can be set for incoming e^+e^- (or $u\bar{u}, d\bar{d}$) pairs. It is obviously unable to tackle experimental selection.
- For `tau-reweight-test.cxx` event re-weighting is demonstrated (LHE or HepMC format can be used) and for each event, two variants of Born are calculated. That is why flag `keyGSW` can not be set once; method `calculateWeightFromParticlesH()` is executed twice⁸ and ratio of the result is used.
At the beginning `EWanomInit` (defined locally in demo) is called and defines initialization variant with the help of `ExtraEWparamsSet()` method.
Next, for each event in the loop, `EWreInit` (it is expected to be adjusted by the user) re-initializes `keyGSW` and other parameters, with the, otherwise dummy, call on `sigbornsdelt`.
- One should note that `sigbornsdelt` call in `tau-reweight-test.cxx` returns dummy variable. The call is to pass `keyGSW` only. Returned value is used in `Dizet-example/table-parsing-test.cxx` though.
- In all the code of `src/ew_born.cxx` and `src/tau_reweight_lib.cxx` the `keyGSW` is not used. Corresponding routines are EW variants independent.

The `src/initwsw.f` is the file where routines for calculating Effective- and/or EW Improved-Born are placed.

In the `src/nonSM.cxx` file, the method `default_nonSM_bornZ()` resides. The class data member variable `m_keyGSW` is used for `keyGSW`, it is accessed with the help of the `keyGSWGet(keyGSW)` method; options are collected in Table 13. In Table 12 names of variables corresponding to the form-factors, introduced in Eq. (1) of Improved Born, which are also used in KKMC and in `Dizet-example` scripts of `TauSpinner`, are explained. These form-factors are used when `t_bornew_` calculation is invoked.

From the point of view of EW calculations most of the variants are set and stored in `EWtables.cxx`. In particular class/file variable `m_keyGSW` is stored among other variables of initialization. To access or modify `ExtraEWparamsGet` and `ExtraEWparamsSet` are prepared. These parameters used in `initEWff` passed with `ExtraEWparamsGet` in particular `keyGSW` is passed to `initwkswdelt_`

⁸The `getWtNonSM()` returns weight for correction with respect to calculation of default SM calculation as initialized in `tauola` universal interface. It may be also suitable to activate call on `EWreInit(1/2)`, for both variants of `calculateWeightFromParticlesH()` calculation. The `EWreInit(1/2)` is expected to be adjusted by the user to actual needs.

In the `EWtables.cxx`, the code for `sigbornswdelt` and `AsNbornswdelt` are stored. Through these methods `keyGSW` is passed to `t_bornnew_`. The `AsNbornswdelt`; a near clone of `sigbornswdelt`, is used in drawing scripts for asymmetries.

It is important to note, that the functions `t_born` and `t_bornnew` which are used in `tauola` universal interface [54] and in `TauSpinner`, are normalized to lowest order Born cross section, of photon exchange only and mass effects excluded. That means $\frac{d\sigma_{Born}^{qq}}{d\cos\theta}(s, \cos\theta, p)$ is multiplied by $\frac{2s}{\pi\alpha^2}$ ($\alpha = \alpha_{QED}(0)$). Thus, Born expression used in the weight calculations should approach $q_f^2 q_l^2 (1 + \cos^2\theta)$ at low energies. This condition, defines normalization for the EW-improved (or other e.g. non SM variant) of user provided Born⁹. This is important if weights are used to relate cross sections obtained from `t_born` and `t_bornnew`. It is of no importance if only spin weight or weight based solely on user provided Born is used. This reference `t_born` of *Effective Born* (inherited from `Tauola`) can be easily modified/replaced by the user, as well as is the case with independently initialized `t_bornnew` of *Improved Born*.

In `TauSpinner` option to improve precision of generated MC events and reweight from “fixed” to “running” width propagator, see Appendix D for explanation, is available. For that `TauSpinner` initialization with `KEYGSW=11`, `KEYGSW=10` and `KEYGSW=2` is prepared. For `KEYGSW=11`, `KEYGSW=12` and `KEYGSW=13` results corresponding to Effective Born, variants `v0`, `v1`, `v2` respectively can be obtained, see Table 13. Let us explain now meaning of all other `sigbornswdelt(mode, ID, s, cc, SWeff, DeltSQ, DeltV, Gmu, alfinv, AMZ00, GAM00, KEYGSW)` input parameters. `mode` can be set to 0 or 1. In the second case `SWeff`, `AMZ00`, `GAM00` for $\sin^2\theta_W^{eff}, M_Z, \Gamma_Z$ will be overwritten with values stored in EW tables calculated with the `DIZET` library. `ID=0,1,2` denotes that calculation is performed respectively for outgoing lepton or down/up quark pair. The `s`, `cc` denote Mandelstam variable and scattering angle. Anomalous coupling δ_{S2W} and δ_V of [13] Appendix B, are initialized with `DeltSQ`, `DeltV` respectively, finally also $G_F, 1/\alpha$ with `Gmu`, `alfinv`. The `AsNbornswdelt()` feature the same set of input parameters, but returns difference for cross section of forward and backward hemispheres instead of the sum.

For important technical details, `README` files and comments in the code of the distribution tar-ball [53] can be helpful.

C Initialization of variants for EW Improved Born

In the previous appendix we have completed presentation of some easy to activate in `TauSpinner` options. In many cases, it is sufficient to change some well defined keys and/or input parameters such as Z boson mass or some couplings. This of course shifts the results. The σ^{tot} , A_{FB} and P_t predictions at the Z -pole are collected in Table 14, for incoming e^+e^- , up or down quarks.

One can see that some options e.g. `KEYGSW=0, 2, 4, 10` are prepared for technical tests, rather than for evaluation of physics ambiguities, while other options are more useful. All these options are useful for test of particular parts of EW predictions obtained with a given version of EW form-factors. This supplements discussed earlier options of EW form-factors initialization, see Appendix A.1 and Table 5. Further, of more historical nature tests, with EW form-factors calculated with older versions of EW `DIZET` library presented in Appendix E, are collected in Fig. 8 and Table. 4. Results of the present Appendix are to supplement discussion of reliability and limitation of the Effective Born variants as compared with Improved Born, in general and in the context of particular applications.

The Effective Born, variants `v0`, `v1`, `v2`, require change of input parameters. Then, `mode=0` and `KEYGSW` at 11, 12 or 13 should be respectively set. One should notice some shifts of Table 14 results with respect to the ones presented e.g. in Tables 2, 3. Note, that we do not average over energy ranges and incoming quark flavours now.

D The s -dependent Z -boson width

In formula (1) for the definition of Z propagator running width is used:

$$\chi_Z(s) = \frac{1}{s - M_Z^2 + i \cdot \Gamma_Z \cdot s / M_Z}. \quad (10)$$

The form-factors of eq. (1) are calculated for the on mass-shell (nominal) value of M_Z . The introduction of so-called s -dependent width is equivalent to partial resummation to higher orders of dominant loop correction: the boson s -dependent self-energy. In fact such resummation, running Z width, was used in many analyses of LEP I era.

However, in Monte Carlos and strong interaction calculations of LHC era, the Z propagator of constant width is often used:

$$\chi'_Z(s) = \frac{1}{s - M_Z^2 + i \cdot \Gamma_Z \cdot M_Z}. \quad (11)$$

One can ask the question, how analytic forms of (10) and (11) translate to each other. In fact, this well known translation is known at least since Ref. [55] published more than 30 years ago, but let us readdress it for the reference again. From Eq. (10),

⁹The method for non SM Born can be replaced with the pointer to the one of user choice.

Table 13: Initialization variants for non-standard Born of quark level Drell Yan $2 \rightarrow 2$ processes. It can be used to impose with the event weight EW loop effects on event samples. Variants are steered by the `keyGSW` parameter. Corresponding code is stored in: (A) - `INITWKSDELTA`, (B) - `T_BORNEW` and (C) - `EWtables.cxx`. Fixed, running and fixed rescaled Γ_Z correspond respectively to Eqs. (10), (11) and (12). Further combination of options can be set by the simple re-coding. The initialization of effective Tauola Born is not affected by these options. It is performed elsewhere. For `KEYGSW=11,12,13`, when `mode=0` results of Effective Born variants `v0`, `v1`, `v2` can be obtained.

KEYGSW	A: VVCor	B: propagator	C: form-factors
0	1	photon propagator off, fixed Γ_Z	all FFi= 1
1	on	running Γ_Z ,	all FFi from EW tables
2	1	fixed Γ_Z	all FFi= 1
3	1	running Γ_Z	all FFi= 1 but FF6= $\Pi_{\gamma}(M_Z^2)$
4	1	running Γ_Z	all FFi= 1 but FF6, FF1= $\rho_{\ell f}(M_Z^2, -M_Z^2/2), \Pi_{\gamma}(M_Z^2)$
5	1	running Γ_Z	all FFi from EW tables calculated at $(M_Z^2, -M_Z^2/2)$
10	1	fixed Γ_Z , rescaled	all FFi= 1
11	1	running Γ_Z	all FFi= 1, can be used for Effective Born v0
12	1	running Γ_Z	FFi set as for Effective Born v1
13	1	running Γ_Z	FFi set as for Effective Born v2

Table 14: Numerical results for initialization variants as explained in Table 13. Numerical results for `v0`, `v1`, `v2` are also provided, then in addition to `KEYGSW=11,12` or `13`, input parameters for `sigbornswdelt()`, `AsNbornswdelt()` need to be adjusted and `mod=0`. The $\alpha(M_Z^2)/\alpha(0)$ factors entering cross sections normalization are dropped out from the σ^{tot} ratios.

KEYGSW	$\frac{\sigma_{tot}^{e^+e^-}(M_Z)}{\sigma_{tot\ improved}^{e^+e^-}(M_Z)}$	$P_{\tau}^{e^+e^-}(M_Z)$	$A_{FB}^{e^+e^-}(M_Z)$
0	0.989939	0.1463264	0.0161546
1	1.000000	0.1449616	0.0177039
2	1.000736	0.2093134	0.0330312
3	1.001438	0.2094436	0.0349617
4	1.011539	0.2093809	0.0344227
5	1.000001	0.1449558	0.0176505
10	1.002227	0.2093154	0.0330336
11	1.000736	0.2093134	0.0330312
11 v0	0.9899340	0.1463264	0.0161546
12 v1	0.9999098	0.1463351	0.0161556
13 v2	0.9999098	0.1463351	0.0161556

KEYGSW	$\frac{\sigma_{tot}^{u\bar{u}}(M_Z)}{\sigma_{tot\ impr.}^{u\bar{u}}(M_Z)}$	$P_{\tau}^{u\bar{u}}(M_Z)$	$A_{FB}^{u\bar{u}}(M_Z)$	$\frac{\sigma_{tot}^{d\bar{d}}(M_Z)}{\sigma_{tot\ impr.}^{d\bar{d}}(M_Z)}$	$P_{\tau}^{d\bar{d}}(M_Z)$	$A_{FB}^{d\bar{d}}(M_Z)$
0	0.989244	0.146859	0.073530	0.988081	0.1471353	0.1032379
1	1.000000	0.146990	0.074664	1.000000	0.1476778	0.1038546
2	1.009430	0.209984	0.109447	1.003882	0.2103266	0.1483706
3	1.009759	0.210529	0.110548	1.003976	0.2107218	0.1488000
4	1.020676	0.210387	0.110274	1.015833	0.2106413	0.1487130
5	0.999999	0.146974	0.074633	0.999999	0.1476667	0.1038425
10	1.010939	0.209986	0.109449	1.005384	0.2103272	0.1483712
11	1.009430	0.209985	0.109447	1.003882	0.2103266	0.1483706
11 v0	0.989244	0.146859	0.073530	0.988081	0.1471353	0.1032379
12 v1	0.999244	0.146863	0.073532	0.998087	0.1471360	0.1032383
13 v2	1.000127	0.146863	0.073573	1.000039	0.1471361	0.1032550

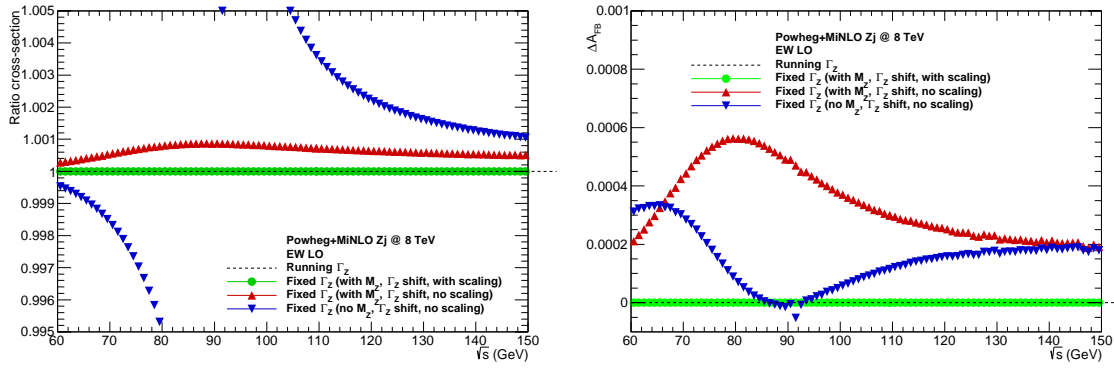


Figure 9: Ratio of the cross sections (left) and ΔA_{fb} (right) for for EW LO but different form of Z-boson propagator, see text. The MC $pp \rightarrow Zj$; $Z \rightarrow l^+l^-$ events were used for estimations.

we obtain Eq. (11) if the following redefinitions are used

$$\begin{aligned}
 \chi_Z(s) &= \frac{1}{s(1 + i \cdot \Gamma_Z/M_Z) - M_Z^2} \\
 &= \frac{(1 - i \cdot \Gamma_Z/M_Z)}{s(1 + \Gamma_Z^2/M_Z^2) - M_Z^2(1 - i \cdot \Gamma_Z/M_Z)} \\
 &= \frac{(1 - i \cdot \Gamma_Z/M_Z)}{(1 + \Gamma_Z^2/M_Z^2)} \frac{1}{s - \frac{M_Z^2}{1 + \Gamma_Z^2/M_Z^2} + i \cdot \frac{\Gamma_Z M_Z}{1 + \Gamma_Z^2/M_Z^2}} \\
 &= N'_Z \frac{1}{s - M_Z'^2 + i \Gamma'_Z M'_Z} \\
 M'_Z &= \frac{M_Z}{\sqrt{1 + \Gamma_Z^2/M_Z^2}} \\
 \Gamma'_Z &= \frac{\Gamma_Z}{\sqrt{1 + \Gamma_Z^2/M_Z^2}} \\
 N'_Z &= \frac{(1 - i \cdot \Gamma_Z/M_Z)}{(1 + \Gamma_Z^2/M_Z^2)} = \frac{(1 - i \cdot \Gamma'_Z/M'_Z)}{(1 + \Gamma_Z'^2/M_Z'^2)} \quad (12)
 \end{aligned}$$

The s -dependent width in Z propagator translates into mass and width shift and introduction of the complex factor in front of the constant width Z propagator. This last point is possibly least trivial as it effectively means redefinition of Z coupling. That is why it can not be understood as parameter rescaling. It points to present in higher order relations between vacuum polarization and vertex. Most of the changes are due to the term Γ_Z^2/M_Z^2 except of the overall phase which result from $1 - i \cdot \Gamma_Z/M_Z$ factor and which change the $\gamma - Z$ interference. The shift in M_Z is by about 34 MeV downwards, and the shift in Γ_Z by 1 MeV, due to the reparametrisation of the Z-boson propagator.

In Figure 9 shown is comparison of the cross sections and A_{fb} , between different implementations of $\chi_Z(s)$. Dashed line of reference corresponds to using formula (10). Green line to complete formula (12). Red line corresponds to formula (12) but without N'_Z scaling and blue line to formula (11), with nominal M_Z and Γ_Z .

It is common for LHC MC generators to use formula (11) for Z propagator, with M_Z and Γ_Z of nominal, on-mass-shell values. Numerically this is better approximation than with shifted M_Z and Γ_Z but N'_Z missing. This observation is true both for EW LO and EW corrected calculations; for cross section and A_{FB} . Quantitative estimates are collected in Tables 15 and 16.

Note that when options of “running Γ_Z ” and “fixed Γ_Z ” are compared, the same EW corrections in both cases tuned to “running Γ_Z ” convention are used. It is beyond the scope of the paper to investigate, how NLO+HO corrections, calculated with the fixed width/ pole mass convention, gradually mitigate (as they should) discrepancy observed at EW LO level between Eq. 10 and Eq. (12) definition of Z propagator without N'_Z included.

Table 15: Ratio of the cross sections (σ), calculated with different form of Z-boson propagator and integrated over outgoing lepton pair mass windows. It is shown for EW LO and EW NLO+HO predictions of $O(\alpha(0))$ EW scheme for pp collisions at 8 TeV center of mass energy, while EW NLO+HO corrections are tuned to running Γ_Z convention.

$\sigma(\text{Fixed})/\sigma(\text{Running})$ m_{ee} ranges (in GeV):	90.5 – 91.5	89 – 93	60 – 81	81 – 101	101 – 150
at EW LO:					
with M_Z, Γ_Z shift, no N'_Z	1.00087	1.00087	1.00062	1.00086	1.00071
no M_Z, Γ_Z shift, no N'_Z	0.99620	1.00074	0.99716	0.99977	1.00392
at EW NLO+HO:					
with M_Z, Γ_Z shift, no N'_Z	1.00113	1.00085	1.00043	1.00083	1.00075
no M_Z, Γ_Z shift, no N'_Z	0.99746	1.00122	0.99719	1.00013	1.00392

Table 16: Difference of A_{fb} calculated for different form of Z-boson propagator and for integrated outgoing lepton pair mass windows. It is shown for EW LO and EW NLO+HO predictions of $O(\alpha(0))$ EW scheme for pp collisions at 8 TeV center of mass energy, while EW NLO+HO corrections are tuned to running Γ_Z convention.

$A_{fb}(\text{Running}) - A_{fb}(\text{Fixed})$ m_{ee} ranges (in GeV):	90.5 – 91.5	89 – 93	60 – 81	81 – 101	101 – 150
at EW LO					
with M_Z, Γ_Z shift, no N'_Z	-0.00048	-0.00047	-0.00047	-0.00047	-0.00030
no M_Z, Γ_Z shift, no N'_Z	-0.00006	-0.00026	-0.00012	-0.00040	-0.00005
at EW NLO+HO					
with M_Z, Γ_Z shift, no N'_Z	-0.00053	-0.00053	-0.00052	-0.00053	-0.00024
no M_Z, Γ_Z shift, no N'_Z	-0.00007	-0.00030	-0.00026	-0.00048	-0.00004

E Versions of DIZET library

In the KKMC distribution tar-ball, explained in Ref. [56], the code for calculation of EW corrections is stored in directory `KK-all/dizet`. The program stored in that directory calculates EW form-factors and writes them into ASCII format text files. To change the version of the form-factors, requires simply use of these tables calculated with different version of library or with different set of initialization parameters. In parallel to program stored in `KK-all/dizet` which calculates EW form-factors as stored with Ref. [57] the following new ones, `dizet-6.42-cpc`, `dizet-6.42` and `dizet-6.45` were prepared and can be used following old instruction of KKMC documentation. There was only one change introduced, convenient for table reading by the `TauSpinner` package [13], the table write format for EW form-factors was modified to `KK-all/dizet/BornV.h` and if tables are used with KKMC the original one of `KK-all/bornv/BornV.h` file should be re-installed. This is true for all mentioned above `DIZET 6.xx` variants.

- `DIZET 6.21 (dizet)` is distributed with KKMC through CPC EW corrections and in particular vacuum polarization was not updated for backup compatibility. This version of library is documented in [17]. Note that upgrades of EW corrections within LEP experiments were not always well documented. This is in particular true for the photon vacuum polarization $\Pi_{\gamma\gamma}(s)$.
- `DIZET 6.42 (dizet-6.42-cpc)` as in published ZFITTER [32]. This is the last published/archived version of `DIZET` code. Note that as a default $\Pi_{\gamma\gamma}$ from ref [33] is still mentioned but obviously it was upgraded for the final versions of LEP data analysis of Ref. [2].
- `DIZET 6.42 (dizet-6.42)` with $\Pi_{\gamma\gamma}$ updated to `hadr5n17_compact.f` of Ref. [25]. Parametrization taken from author web page, dated Oct 8 02:19:56 2017.
- `DIZET 6.45 (dizet-6.45)` VERSION 6.45 (30 Aug. 2019) with the vacuum polarization code and fermionic two loops corrections, `AMT4` flag upgraded by `DIZET` authors themselves.

Comparison of results for these versions are given in Fig. 8 and in Table 4.